Preprints.org

Article

Not peer-reviewed version

Non-Cumulative, Size-Specific Calibration of Low-Cost Particulate Matter Sensors Under Simulated Construction Drilling Events

Askarov Komiljon and Jae-ho Choi *

Posted Date: 17 April 2026

doi: 10.20944/preprints202604.1260.v1

Keywords: particulate matter; construction dust monitoring; low-cost PM sensors; sensor performance evaluation; size-specific correction factor

Preprints.org is a free multidisciplinary platform providing preprint service that is dedicated to making early versions of research outputs permanently available and citable. Preprints posted at Preprints.org appear in Web of Science, Crossref, Google Scholar, Scilit, Europe PMC.

Copyright: This open access article is published under a Creative Commons CC BY 4.0 license, which permit the free download, distribution, and reuse, provided that the author and preprint are cited in any reuse.

Preprints.org (www.preprints.org) | NOT PEER-REVIEWED | Posted: 17 April 2026 doi:10.20944/preprints202604.1260.v1

Disclaimer/Publisher's Note: The statements, opinions, and data contained in all publications are solely those of the individual author(s) and contributor(s) and not of MDPI and/or the editor(s). MDPI and/or the editor(s) disclaim responsibility for any injury to people or property resulting from any ideas, methods, instructions, or products referred to in the content.

Article

Non-Cumulative, Size-Specific Calibration of Low-Cost Particulate Matter Sensors Under Simulated Construction Drilling Events

Askarov Komiljon and Jae-ho Choi *

ICT Integrated Safety Ocean Smart Cities Engineering Department, Dong-A University, S12-401-1, 550 Bungil 37, Nakdong-Daero, Saha-Gu, Busan, 49315, South Korea

* Correspondence: jaehochoi@donga.ac.kr

Abstract

Urban construction activities are recognized as significant contributors to particulate matter (PM) emissions; however, the accurate real-time monitoring of size-resolved PM fractions presents a formidable challenge. Traditional low-cost PM sensors predominantly report cumulative concentrations, which obscures the distinct health and regulatory significance of PM1, PM2.5, and PM10. This study systematically evaluates the performance of two low-cost sensors—PMS5003 and Sniffer4D, utilizing non-cumulative measurements obtained under controlled laboratory conditions designed to simulate construction PM generated from concrete slab drilling. Sensor performance was rigorously analyzed using Pearson correlation coefficients, standard deviation, and mean percentage differences. Six correction models—Linear Regression, Polynomial Regression, Random Forest (RF), XGBoost, Artificial Neural Network (ANN), and Kalman Filter—were independently developed for each PM size fraction to enhance measurement precision. Findings reveal that RF and ANN consistently provided the most accurate corrections, particularly for PM1 and PM2.5, with RF achieving a coefficient of determination (R^2) > 0.89 for PM1 and R^2 > 0.87 for PM2.5 at the 50-second duration. This investigation introduces a size-resolved correction framework specifically designed for construction environments, thereby advancing the capability of low-cost sensors to enable accurate particle-specific exposure assessments.

Keywords: particulate matter; construction dust monitoring; low-cost PM sensors; sensor performance evaluation; size-specific correction factor

1. Introduction

Urban air quality is increasingly compromised by rapid urbanization, growing vehicular traffic, and intensive construction activities. Notably, the construction sector substantially contributes to particulate matter (PM) pollution, particularly PM10 (particles ≤10 μm), PM2.5 (≤2.5 μm), and ultrafine PM1 (≤1 μm), posing significant risks to public health. For instance, construction activities in London account for approximately 30% of PM10 and 8% of PM2.5 emissions [1]. Similarly, in South Korea, fugitive dust from construction sites represents roughly one-third of total PM10 emissions [2]. Key dust-generating activities include demolition, excavation, material transportation, and concrete processing, significantly elevating localized PM concentrations[1,2]. These emissions are especially concerning in densely populated urban areas, affecting not only construction workers but also nearby residents, leading to heightened risks of respiratory and cardiovascular diseases [3]. Vulnerable populations such as children, the elderly, and individuals with pre-existing conditions disproportionately experience adverse health outcomes associated with PM exposure [4,5].

Regulatory bodies have responded by implementing stringent PM limits and dust control measures at construction sites to safeguard public health. Agencies such as the U.S. Environmental Protection Agency (USEPA) and the European Union (EU) mandate adherence to established PM10

© 2026 by the author(s). Distributed under a Creative Commons CC BY license.

Preprints.org (www.preprints.org) | NOT PEER-REVIEWED | Posted: 17 April 2026 doi:10.20944/preprints202604.1260.v1

and PM2.5 standards during construction operations [6,7]. However, compliance remains challenging as uncontrolled construction activities frequently yield PM concentrations significantly exceeding recommended health guidelines. For instance, Khan et al. (2021) [8] documented PM2.5 and PM1 mean exposure levels of 471 μg/m³ and 59 μg/m³, respectively, during concrete mixing, substantially surpassing WHO guidelines (World Health Organization) and underscoring the critical need for real-time PM monitoring and mitigation strategies in construction settings. Cheriyan et al.(2020),[9] highlighted existing Environmental Impact Assessments (EIAs) often fail to capture activity-level emissions like drilling, cutting, or manual mixing, contributing significantly to fine particle generation in construction sites, thus he highlighted the need for real-time, location-based PM monitoring that distinguishes particle sizes is essential to developing targeted control strategies.

Conventionally, gravimetric and optical instruments such as Federal Reference Method (FRM) samplers and Federal Equivalent Method (FEM) monitors (e.g., beta attenuation monitors and TEOMs) have been employed for PM monitoring, providing highly accurate measurements. Nevertheless, their high costs, bulkiness, and extensive maintenance requirements limit their widespread deployment, resulting in sparsely distributed stationary monitoring stations being unable to effectively capture the spatial variability of PM around dynamic construction sites [10]. Consequently, these methods can inadequately represent actual personal exposure in microenvironments characterized by heterogeneous dust distributions [11,12].

The advent of low-cost particulate matter sensors (LCPMS) has significantly enhanced air quality monitoring by providing affordable, portable, and scalable alternatives. Employing optical light-scattering principles, these sensors facilitate dense networks and mobile monitoring deployments [12]. Numerous studies have demonstrated a high correlation (>90% Coefficient of Determination (R^2)) between certain modern optical LCPMS (e.g., Plantower PMS5003, Alphasense OPC-N3) and reference instruments under specific conditions [13,14]. The capability for simultaneous real-time data collection using UAV-mounted sensors and other spatially distributed PM measurement systems enables high-resolution spatial mapping of PM emissions, which is crucial not only for the immediate evaluation of PM control measures but also for achieving more precise PM reduction through the application of current PM mitigation technologies, ultimately safeguarding occupational and residential health [11].

Despite their promising potential, LCPMS exhibit notable limitations in data accuracy and reliability, particularly when deployed in complex, high-dust environments characteristic of construction sites. Laboratory evaluations have consistently demonstrated that sensor performance varies significantly depending on particle size, with a tendency to undercount larger particles (>5 μm) and to inconsistently detect coarse particles due to their irregular shapes and heterogeneous compositions [14,15]. Moreover, environmental factors such as particle composition, relative humidity, temperature fluctuations, and ambient airflow introduce additional biases and variability in sensor readings [16,17]. Consequently, calibration conducted solely under clean ambient conditions is insufficient for reliably predicting sensor performance in real-world, high-dust environments.

These sensor performance limitations underscore a critical research gap: the need to establish particle size-specific correction factors for LCPMS when applied to construction-generated PM. Unlike typical urban aerosols, construction-generated PM is composed predominantly of larger, irregularly shaped particles such as concrete dust, soil, and gypsum, which pose particular challenges to optical sensors originally calibrated for detecting fine combustion-derived aerosols [18–20]. Additionally, most prior sensor validation studies have focused on aggregate PM2.5 or PM10 measurements without independently verifying the accuracy of PM1, PM2.5, and PM10 channels [13,14,21].

Recent studies have highlighted the increased health risks associated with fine PM, revealing that the relative risk posed by PM1 can be up to 66 times greater than that of PM10 under identical exposure conditions [22,23]. For example, during hollow block drilling operations, the hazard index for PM exposure (HIPM) was calculated at just 0.12, whereas the index based on toxic substance

© 2026 by the author(s). Distributed under a Creative Commons CC BY license.

Preprints.org (www.preprints.org) | NOT PEER-REVIEWED | Posted: 17 April 2026 doi:10.20944/preprints202604.1260.v1

exposure (HITS)—a more appropriate metric for ultrafine particles—reached as high as 8.25. This stark contrast highlights the disproportionate health burden imposed by smaller particle sizes. As it is well established that PM10 tends to deposit in the upper respiratory tract, while PM2.5 and PM1 penetrate more deeply into the lungs and even enter the bloodstream, there is a pressing need for the development of rigorous, size-specific calibration protocols in PM monitoring and risk assessment [22,24,25].

Despite growing interest in low-cost PM sensor calibration, three critical gaps remain. First, most studies evaluate sensors under ambient urban conditions rather than high-intensity, short-duration construction emissions. Second, existing calibration approaches often rely on cumulative PM reporting, limiting size-specific exposure assessment. Third, the stability of correction models across different emission durations remains poorly understood. This study addresses these limitations by implementing a size-resolved, non-cumulative calibration framework specifically designed for construction drilling events at multiple time scales under controlled laboratory conditions, simulating authentic construction-generated PM from concrete slab drilling. By enhancing the accuracy and reliability of LCPMS in capturing size-specific PM concentrations, this research aims to support more effective monitoring practices, regulatory compliance, and health protection strategies within the construction sector.

2. Literature Review

This literature review critically evaluates recent advancements and persistent limitations in the performance assessment, and calibration strategies of LCPMS, with particular emphasis on their ability to distinguish and accurately quantify PM1, PM2.5, and PM10 across ambient and construction-specific environments.

2.1. Evaluation of LCPMS

Initial studies on LCPMSs primarily evaluated their performance under general urban and rural ambient conditions. Zeng et al.(2018), [26] tested a Plantower PMS3003 sensor in both low-pollution (United States) and high-pollution (India) environments. They observed that sensor accuracy improved at higher particle concentrations and with longer averaging intervals. For example, uncorrected hourly PM2.5 readings showed very large errors (up to 201% deviation from reference) under clean-air conditions, whereas 24-hour averaging in high-PM environments reduced error to about 9%. Importantly, variability in relative humidity explained up to 30% of the sensor's output variance and recommended a quadratic calibration model to correct non-linear response effects at high PM levels.

Tryner et al. (2020), [17] expanded LCPMS validation to consider aerosol type and sensor aging. In a controlled laboratory study, they compared three optical sensors (Plantower PMS5003, Sensirion SPS30, and Novafitness SM-UART-04L) against reference instruments while introducing different aerosol compositions and exposing sensors to extended operation. All three sensors correlated strongly with the reference mass concentrations ($R^2 \geq 0.97$), indicating good baseline accuracy. However, differences emerged in size-resolved performance and long-term stability. The PMS5003 tended to overestimate particle mass and showed greater signal drift over time, whereas the SPS30 provided more stable readings and better discrimination for specific size fractions over the aging period. These results highlighted that particle characteristics (such as size and composition) can influence sensor response and that some LCPMS models (like the SPS30) may be inherently more stable or accurate over time than others.

For indoor environments, recent work has evaluated whether LCPMS can reliably monitor indoor air quality. Park et al. (2023), [27] assessed the PurpleAir PA-II sensor (which contains dual PMS5003 laser counters) by co-locating it with research-grade instruments (GRIMM optical spectrometer and TSI SidePak) in a controlled indoor setting. The PurpleAir sensors showed excellent consistency with each other and reported accurate PM2.5 concentrations under 100 $\mu g/m^3$, validating their use for low-level indoor PM2.5 monitoring. However, accuracy dropped off significantly for

© 2026 by the author(s). Distributed under a Creative Commons CC BY license.

Preprints.org (www.preprints.org) | NOT PEER-REVIEWED | Posted: 17 April 2026 doi:10.20944/preprints202604.1260.v1

larger particles and higher dust loads: the sensors markedly underestimated concentrations when true indoor PM10 exceeded 100 μg/m³, and they showed inconsistent particle number counts for particles larger than 1 μm. This indicates that, while low-cost units can perform well for fine particulate monitoring indoors, they may require calibration or algorithmic adjustments to reliably measure coarse dust in indoor environments.

Complementary field studies have benchmarked popular low-cost sensors against regulatory-grade monitors in outdoor settings. For instance, Cowell et al.(2022), [13] deployed PMS5003 sensors in an outdoor urban air monitoring network and calibrated them against reference instruments (beta-attenuation monitor and gravimetric samplers). Their field results showed moderate to strong correlations (R^2 0.54–0.72) between the raw PMS5003 readings and reference for PM1, PM2.5, and PM10 concentrations. Nevertheless, performance degraded notably at high ambient humidity (>85% relative humidity), which caused the low-cost sensors to over-count particle mass. The authors addressed this by developing a multi-linear regression correction that included a humidity term, which improved the agreement with reference data (post-correction Pearson R up to 0.91). Even so, the study found evidence of calibration drift over 8 weeks in the field, suggesting that LCPMS units require periodic recalibration to maintain accuracy. In a different outdoor scenario focused on windblown dust, Kaur et al.(2023), [21] evaluated two sensor types—Plantower PMS5003 and Alphasense OPC-N3—during dust storm events in the Salt Lake Valley (Utah). The OPC-N3 (a laser optical particle counter with a larger detection range) outperformed the lower-cost PMS5003, achieving R^2 = 0.87–0.94 for PM10 when compared to an EPA Federal Equivalent Method and GRIMM aerosol spectrometer. By contrast, the PMS5003 severely underestimated PM10 under these harsh conditions (R^2 < 0.5, with root-mean-square errors (RMSE) >30 μg/m³). Applying simple ratio-based correction factors (e.g., using the PM2.5/PM10 ratio) improved PMS5003 performance only modestly. These field studies underscore those environmental factors—especially humidity and aerosol type—can significantly affect sensor readings, and that advanced or size-specific calibration models are often necessary for LCPMS to achieve high accuracy in real-world conditions.

Despite their promise, a critical shortfall of current LCPMS research is the lack of rigorous, non-cumulative, size-specific evaluation of sensor outputs. Kuula et al.(2020), [15] conducted a comprehensive laboratory analysis of several popular sensors' size-selective performance. They found that many LCPMS did not truly adhere to the nominal PM1, PM2.5, and PM10 cutoffs stated by manufacturers. Each low-cost sensor effectively detected particles in only one or two broad size ranges. For example, a given sensor might respond reliably to accumulation-mode particles (0.1–1 μm, reported as "PM1"), but its readings for coarse-mode particles (>2.5 μm) might be highly inaccurate or simply scaled from the finer particles. High-end optical spectrometers, by contrast, can distinguish a dozen or more size bins with calibrated optical algorithms. This limitation of low-cost devices is especially problematic when precise discrimination between PM1, PM2.5, and PM10 is needed.

Although limited research exists on the evaluation of LCPMS specifically in construction environments, the literature highlights a significant gap in assessing sensor performance under controlled conditions that reflect the unique characteristics of construction-generated PM. Unlike ambient or urban PM typically used in sensor validation, construction PM poses distinct challenges. Khan et al.(2021), [8] addressed the evaluation of the Alphasense OPC-N2 sensors under construction environments from construction activity, reporting high inter-sensor correlations—up to 0.96 for PM1 and PM2.5, and 0.76 for PM10 using smoothed averages. Similarly, Cheriyan et al.(2020), [18] evaluated the performance of low-cost sensors—Alphasense OPC-N2 and Sharp GP2Y1010—against a benchmark Kanomax 3443 PM_{10} monitor during construction activity in the laboratory, finding that Alphasense sensors maintained strong correlations above 0.96 and over 99% precision. Although Sharp sensors exhibited reduced sensitivity at lower PM concentrations, they still showed substantial agreement with Alphasense OPC-N2 and benchmark instruments, supporting their potential for monitoring construction PM. Furthermore, most literature reports cumulative particle metrics or total suspended dust, rather than verifying the accuracy of each size fraction group independently. This

© 2026 by the author(s). Distributed under a Creative Commons CC BY license.

Preprints.org (www.preprints.org) | NOT PEER-REVIEWED | Posted: 17 April 2026 doi:10.20944/preprints202604.1260.v1

gap makes it difficult to know how well a sensor's "PM2.5" output, for instance, truly reflects ultrafine particle concentrations versus simply being a fraction of its PM10 measurement.

2.2. Calibration of LCPMS

Beyond performance evaluation, researchers have explored various calibration techniques to improve LCPMS accuracy. A variety of statistical and machine-learning approaches have been applied—most focusing on PM2.5 as the target metric, since it is regulated and widely monitored. For example, Si et al.(2020), [28] co-located PMS5003 sensors with a reference SHARP monitor and tested multiple calibration models, including simple linear regression, multiple linear regression, gradient-boosted trees (XGBoost), and a feed-forward neural network. Calibration using the neural network model reduced the PM2.5 root mean square error (RMSE) from 9.93 μg/m³ (uncalibrated) to 3.91 μg/m³. in addition, in a recent study by Saputra et al.(2025), [29] both linear and polynomial models were employed to calibrate an SPS30 sensor using the decay method. The results indicated that the polynomial model slightly outperformed the linear approach, achieving an R^2 of 0.9994 for PM2.5 and 0.9978 for PM10. This confirms the value of polynomial regression in enhancing calibration accuracy for particulate matter measurements. In another study, Chen et al. (2018), [30] used a feed-forward neural network to calibrate PMS7003 sensor readings against a BAM-1020 reference, demonstrating that incorporating environmental factors (temperature and humidity) could raise the coefficient of determination (R^2) from 0.62 to 0.91. Advanced time-series models have also been explored: Park et al. (2021), [31] introduced a hybrid deep learning model (combining a dense neural network with a long short-term memory sequence model) to calibrate indoor PM2.5 data, achieving a high R^2 of 0.93. Yadav et al. (2022), [32] proposed a few-shot meta-learning framework (MAML) to rapidly calibrate PM2.5 sensors in data-sparse scenarios, reporting a 32% reduction in error with minimal new training data. These studies collectively demonstrate that machine learning can substantially improve LCPMS accuracy for PM2.5 under various conditions.

However, all of the above calibration efforts share critical limitations: they focus almost exclusively on PM2.5 and do not evaluate or adjust the sensors' performance for PM1 and PM10. This narrow scope overlooks the possibility that a sensor's errors for fine to coarse particles may behave differently. In addition, most calibrations were performed in urban ambient air environments; few considered extreme conditions like construction sites where particle size distributions skew many courses (PM10-rich) and concentrations can be intermittently very high. The calibration models developed for typical urban aerosols may not generalize well to PM-laden construction air. Indeed, when multiple PM size fractions are measured, researchers often treat the data cumulatively – for instance, correcting only PM2.5 and assuming those corrections apply to PM10 – or applying a uniform model across all particle sizes. Such approaches can mask important differences in sensor response between fine and coarse modes.

A smaller group of recent studies has begun to address the calibration of LCPMS for multiple PM size fractions, including PM1 and PM10. Raheja et al. (2023), [33] conducted one of the most comprehensive evaluations of this kind, using a network of low-cost sensors in Accra (Ghana) and testing several calibration models (Multiple Linear Regression, Gaussian Mixture Regression, Random Forest, and XGBoost) across PM1, PM2.5, and PM10 channels. Their findings indicate that no single method performs best for all particle sizes: for example, in their data, Random Forest provided the highest accuracy for PM1, whereas XGBoost yielded the best PM10 predictions. This reinforces that sensor behaviour varies with particle size and that calibration might need to be size-specific.

Laboratory research by Huang et al. (2021), [34] demonstrated the benefit of size-tailored calibration: using a chamber with known test aerosols, they calibrated a Plantower PMS A003 sensor for PM1, PM2.5, and PM10 by accounting for each aerosol's refractive index and density. The resulting models achieved normalized mean absolute errors below 5% for all three size fractions, dramatically improving accuracy by adjusting for particle optical properties.

© 2026 by the author(s). Distributed under a Creative Commons CC BY license.

Preprints.org (www.preprints.org) | NOT PEER-REVIEWED | Posted: 17 April 2026 doi:10.20944/preprints202604.1260.v1

In a more applied context, Hashmy et al. (2021), [35] developed a modular IoT-based system that simultaneously processes and corrects multi-size data from low-cost sensors. Their approach used machine-learning sub-models for each size fraction and reported consistent performance across PM1, PM2.5, and PM10 in preliminary tests. Likewise, Rueda et al. (2023), [36] analyzed long-term field data from co-located low-cost sensors and found much higher variability in the sensors' PM10 readings than in PM1 or PM2.5. They concluded that coarse particle measurements are the least reliable and require separate, robust calibration since the low-cost devices could not accurately capture rapid changes in the coarse fraction. Christakis et al. (2024), [37] demonstrated that applying a Kalman filter to sensor data improved correlation coefficients with reference instruments from 0.50–0.68 to 0.89–0.92 and reduced error indicators such as MSE and RMSE. Its low computational burden and suitability for real-time implementation make it particularly advantageous for IoT-based air quality monitoring systems using low-cost sensors. Overview of previous LCPMS evaluation and calibration studies provided in Supplementary Table S1.

2.3. Summary of Previous Studies

These gaps underscore the need for a systematic, laboratory-based evaluation of LCPMS performance under controlled exposure to construction-generated PM. There is a particular need to develop non-cumulative calibration protocols that assess PM1, PM2.5, and PM10 accuracy independently and apply tailored correction factors for each size class. Addressing this knowledge gap, the present study aims to generate particle-size–specific calibration models for low-cost sensors from concrete slab drilling activity in construction site environments, thereby enhancing the precision and applicability of LCPMS in occupational air quality monitoring. While the findings will primarily guide researchers and practitioners in improving sensor accuracy for specific particle sizes, they will also inform more effective PM management strategies and policies by providing data that distinguish the health impacts associated with each particle size.

3. Materials and Methods

This study aims to evaluate the performance of low-cost particulate matter sensors (LCPMS) under simulated construction-generated PM conditions and to develop size-specific correction factors to enhance their field applicability. The methodology is structured into four interlinked phases, as illustrated in Figure 1:

1. Laboratory evaluation of PM emissions through controlled concrete drilling,
2. Performance assessment using statistical and accuracy-based metrics,
3. Correction factor implementation using advanced machine learning algorithms,
4. Field deployment guidance for reliable LCPMS applications at construction sites.

These phases are logically sequential and methodologically dependent. The first phase (laboratory evaluation) generates foundational data on particulate emissions during controlled construction activity, which serves as the input for the second phase, where the precision, consistency, trend recognition, and accuracy of each sensor are evaluated. Insights from this analysis inform the third phase, where correction models are trained using machine-learning techniques to address size-specific discrepancies and sensor-specific limitations. Finally, non-cumulative findings are used to guide the practical deployment of LCPMS in real-world construction environments, ensuring enhanced data reliability and usability.

To simulate construction-related PM generation in a controlled environment, this study employed a concrete slab drilling activity, replicating common dust-emitting construction processes. The experimental setup was adapted from methodologies established by Cheriyan et al.(2021), [9] and Priyanka et al.(2022), [38]. The laboratory facility measured 6 m × 6 m, with a 4 m × 4 m dust chamber designated for the drilling activity, and the remaining space allocated for equipment setup and data collection systems (see Figure 2a).

© 2026 by the author(s). Distributed under a Creative Commons CC BY license.

Preprints.org (www.preprints.org) | NOT PEER-REVIEWED | Posted: 17 April 2026 doi:10.20944/preprints202604.1260.v1

Three monitoring stations (MS1, MS2, and MS3) were installed equidistantly around the activity zone at 120° intervals to eliminate cross-interference between sensor airflow patterns (see Figure 2b). Each station was equipped with a distinct low-cost PM sensor—PMS5003, OPC-N3, or Sniffer4D—to compare performance under identical environmental conditions. To mitigate environmental biases within the chamber, sensors were placed 1 meter from the wall to prevent particle deflection. A moist adhesive floor mat was installed to reduce particle resuspension, enhancing data integrity.

For correction factor modeling, this study applied five widely adopted algorithms: Artificial Neural Networks (ANN), XGBoost, Random Forest (RF), Kalman Filter, and Linear Regression. These models were trained using lab-generated sensor data to account for known limitations such as non-linear sensor response, baseline drift, and particle-size sensitivity.

Since all tests were conducted in a strictly controlled indoor environment, external environmental factors such as temperature and relative humidity were held constant and not included in the correction model inputs. Further technical details, including correction model configuration, training-validation procedures, and feature engineering, are presented in the following section, Experimental Design and Implementation.

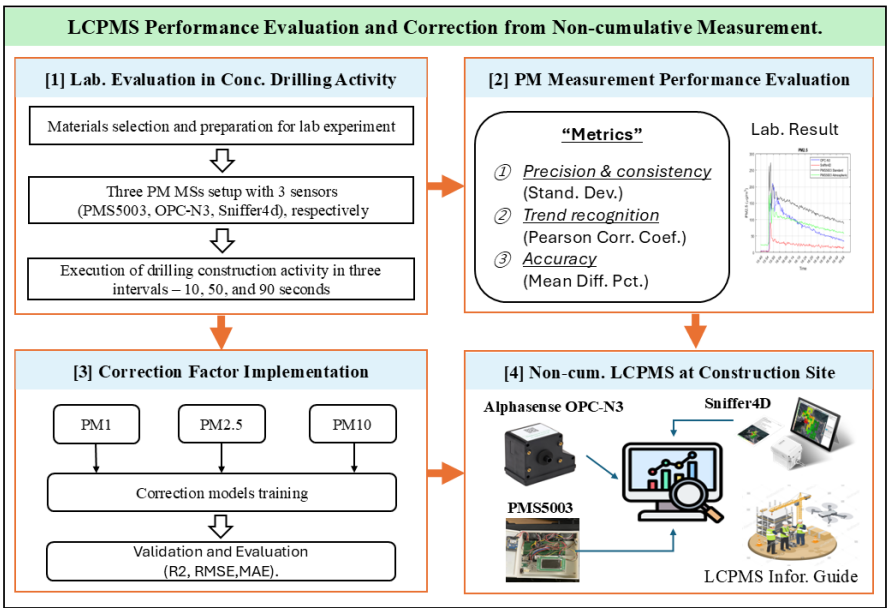

Figure 1. Methodology to evaluate the PM sensors.

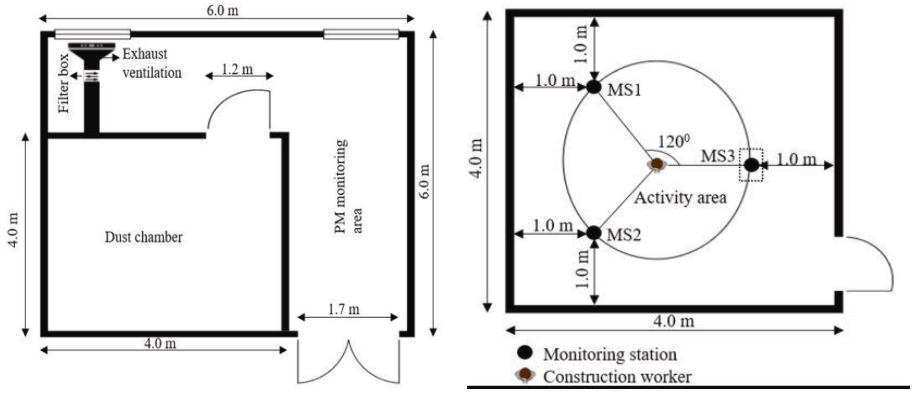

(**a**) Floor plan of laboratory (**b**) Experiment set-up (MSs, Angle, Distance)

Figure 2. Experimental setup in the laboratory to monitor PM emission from a construction activity [38].

© 2026 by the author(s). Distributed under a Creative Commons CC BY license.

Preprints.org (www.preprints.org) | NOT PEER-REVIEWED | Posted: 17 April 2026 doi:10.20944/preprints202604.1260.v1

4. Experimental Design and Implementation

4.1. Sensor Selection Based on Sensor Characteristics

The performance of PM sensors is critical for ensuring LCPMS provides accurate PM monitoring data, especially in environments where precise measurements of PM1, PM2.5, and PM10 are necessary. Table 1 summarizes the key specifications of PMS5003, OPC-N3, and Sniffer4D, incorporating information closely related to the sensor's PM measurement performance from their product data sheets and experimental results obtained during this study. PMS5003 is a compact LCPMS and among the widely used sensors, which costs less than most other dust sensors. PMS5003 sensor produces scattering by using the laser to radiate suspending particles in the air, then collects scattering light to a certain degree, and finally obtains the curve of scattering light change with time. The PMS5003 sensor provides data in two modes standard particle measurement and atmospheric measurement. The former refers to the sensor's condition as produced through standard procedures in the factory, while the latter refers to the sensor's condition adjusted with specific calibration factors for air quality measurement [39].

OPC-N3 is a compact, low-cost sensor that uses light scattering methods for PM measurement listed in the United States Environmental Protection Agency (USEPA) and is widely used in air quality monitoring. One of the key features of the OPC-N3 is its high resolution and accuracy. It provides detailed particle size distribution data across 24 user-defined size bins, allowing users to detect even subtle changes in particle size distribution and the maximum particle count rate is 10,000 particles per second with the capability to measure up to 2,000 ug/m^3 highlighting that OPC-N3 can detect very high level of PM concentrations [40]. The Sniffer4D is an advanced air quality monitoring sensor designed for high-resolution, real-time detection and analysis of various environmental pollutants (PM, CO2, CO, NO2, SO2, O3, and VOCs) depending on the module selected by users, the authors used only the PM module for this study (Soarability, 2024).

Table 1. Comparison of the specifications of the PMS5003, OPC-N3, and Sniffer4D.

Specification	Plantower PMS5003	Alphasense OPC-N3	Sniffer4D
Detection method	Laser scattering	Laser scattering	Laser scattering
Particle size range (μm)	PM1 (0.3~1.0), PM2.5 (1.0~2.5), PM10 (2.5~10)	PM1 (0.35~1), PM2.5 (0.35~2.5), PM10 (0.35~10)	PM1.0 (0.3~1), PM2.5 (0.3~2.5), PM10 (0.3~10)
Particle counting effectiveness	50%@0.3μm, 98%@≥0.5μm	50%@0.3μm, 100%@0.35μm[1)]	50%@0.3μm, 98%@≥0.5μm
Particle Effective Range (μg/m3)	0~500[2)]	0~2,000	0~1,000
Intervals	0.2-2.3s	1-30s	1s[3)]
Humidity	0~99	0 to 95 (non-condensing)	Humidity Correction[4)]
Temp.	-10 to 60 °C (10 °C to 40 °C)[5)]	-10 to 50 ^{0}C	-30 °C to 50 °C
Air flow rate	N/A	5.5 L/min	5 L/min
Calibration	Calibrated with cigarette smoke in Lab.	Calibrated with TSI PM counter	Use algorithm to adjust PM with temp, pressure, humidity

(1) Based on 100% detection efficiency at 0.35μm, 50% at 0.3μm, (2) The Particle Effective Range for PMS5003 is until 500 for PM2.5 standard mode. (3) The formal information is not available, so it is based on the authors' experiment findings, (4) A unique built-in humidity correction algorithm to improve measurement accuracy over a wide range of humidity, (5) Stable region: Max. Error Modulus remains relatively constant at around 10%, indicating a stable consistency.

© 2026 by the author(s). Distributed under a Creative Commons CC BY license.

Preprints.org (www.preprints.org) | NOT PEER-REVIEWED | Posted: 17 April 2026 doi:10.20944/preprints202604.1260.v1

All three sensors utilize the laser scattering method as their detection mechanism, a reliable technique for PM measurement. However, their performance varies based on key specifications. In terms of particle size range, the PMS5003 measures PM in a non-cumulative manner, with PM1 representing particles sized between 0.3 and 1.0 μm, PM2.5 ranging from 1.0 to 2.5 μm, and PM10 ranging from 2.5 to 10 μm. The OPC-N3 cumulatively measures PM, with PM1 representing particles sized between 0.3 and 1.0 μm, PM2.5 ranging from 0.3 to 2.5 μm, and PM10 ranging from 0.3 to 10 μm. Sniffer4D measures PM in a cumulative manner similar to the OPC-N3, with PM1 representing particles sized between 0.3 and 1.0 μm, PM2.5 ranging from 0.3 to 2.5 μm, and PM10 ranging from 0.3 to 10 μm.

The particle-counting effectiveness of the sensors provides valuable insight into their suitability for various PM monitoring applications. For ultrafine particles (0.3 μm), the PMS5003 and Sniffer4D perform equally well, with a detection efficiency of 50%. In contrast, the OPC-N3's performance in this range is less clearly defined. For particles ≥0.35 μm, the OPC-N3 stands out with a perfect detection efficiency (100%), outperforming PMS5003 and Sniffer4D, which achieve 98% efficiency for particles ≥0.5 μm. In general, for sensors utilizing laser scattering, particle counting effectiveness tends to improve as particle size increases. This is attributed to the stronger light scattering generated by larger particles, as described by light scattering physics and MIE scattering theory [20,41]. If these provided facts are accurate, the OPC-N3 sensor is expected to demonstrate measurement performance close to 100% for PM sizes ≥0.35 μm, suggesting its capability for more precise PM measurements.

In terms of measurement range, the PMS5003 and Sniffer4D can measure PM concentrations up to 500 μg/m³, and 1,000 μg/m³, respectively, while the OPC-N3 has an extended range of up to 2,000 μg/m³. This broader range makes the OPC-N3 particularly suitable for environments with high PM concentrations, such as industrial areas or locations experiencing severe pollution. Regarding sampling intervals, the PMS5003 sensor operates in two modes: a stable mode with a reporting interval of approximately 2.3 seconds under steady conditions, and a fast mode with intervals between 200 to 800 milliseconds when detecting rapid changes in particle concentration [39]. On the other hand, the OPC-N3 and Sniffer4D operate with fixed 1-second intervals, enabling consistent and frequent data collection. The OPC-N3 has the highest airflow rate of 5.5 L/min, followed by Sniffer4D at 5 L/min, while PMS5003 does not specify its airflow rate. A higher airflow rate can improve measurement accuracy by sampling a larger volume of air. Overall, this analysis highlights the distinct strengths and limitations of each sensor.

Sniffer4D's calibration using an algorithm ensures superior adaptability to changing environmental conditions, such as temperature and humidity. In contrast, OPC-N3, calibrated with a TSI PM counter, provides high accuracy under standard conditions. PMS5003, calibrated with cigarette smoke, may face limitations in real-world environments with diverse PM sources. Based on a comprehensive review of all the information, the OPC-N3 is deemed a suitable sensor for accurate PM concentration measurements and applications involving high levels of PM emissions. In contrast, the PMS5003 and Sniffer4D are well-suited for general air quality monitoring in urban or residential areas where moderate levels of PM are expected.

4.2. Reference Sensor Selection

For lab. sensor evaluation, a concrete slab drilling activity was chosen to artificially produce the PM emission for sensor performance evaluations as it is one of the tasks generating the largest PM among all construction activities [38]. The OPC-N3 was determined based on the results of performance taken by previous researchers and used as a reference sensor for both laboratory and correction factor implementation of LCPMS. Scientific evidence supports the use of the OPC-N3 as a reliable reference sensor for monitoring PM in laboratory settings. A study by Cheriyan et al.(2022), [18] highlights that the Alphasense OPC-N2 is a reliable low-cost sensor capable of accurately measuring PM10, PM2.5, and PM1 concentrations in construction environments. It demonstrated high sensitivity to fine particles, strong precision among units (>99%), and strong correlation (up to

© 2026 by the author(s). Distributed under a Creative Commons CC BY license.

Preprints.org (www.preprints.org) | NOT PEER-REVIEWED | Posted: 17 April 2026 doi:10.20944/preprints202604.1260.v1

R^2 = 0.96) under stable laboratory conditions. Unlike cheaper sensors like Sharp, the OPC-N2 effectively detected lower PM levels without saturation, making it suitable as a reference sensor in indoor experiments. Kaur et al.(2023a,b), [14,21] demonstrated the OPC-N3's strong performance and consistency against reference-grade instruments. The sensor showed high correlations with FEM PM10 measurements (R^2 = 0.865, RMSE = 12.4 μg/m³) and the GRIMM aerosol spectrometer (R^2 = 0.937, RMSE = 17.7 μg/m³). Using monodisperse Dioctyl sebacate (DOS) particles, the OPC-N3 exhibited accurate size selectivity, a positive bias for mean particle diameter, and a coefficient of variance (CV) below 10%. Sousan et al.(2021), [42] also validated its high linearity (r = 0.99) and precision (CV = 4.4–16%) under various environmental conditions. These studies highlight the OPC-N3's technical advantages, justifying its selection as a reference sensor to evaluate PMS5003 and Sniffer4D in this study.

4.3. Execution of Experiments

The authors manually drilled the concrete slab to analyze the PM concentration generated from construction activity with the PMS5003, OPC-N3, and Sniffer4D sensors. To ensure accurate sensor readings, the sensors were positioned at a 120° angle to the PM source to minimize performance interference and placed at a height of 1.3 m, reflecting the average human breathing height. Additionally, all sensors were located 1 m away from the PM source, as illustrated in Figure 3. For optimal accuracy, sensors should be positioned as close as possible to the PM source, [9].The drilling activity was conducted for 10 seconds, 50 seconds, and 90 seconds, with corresponding observations recorded for 1 hour.

(**a**) Laboratory PM MSs Setup

(**b**) Conc. Slab Drilling Activity

Figure 3. Execution of experiment.

© 2026 by the author(s). Distributed under a Creative Commons CC BY license.

Preprints.org (www.preprints.org) | NOT PEER-REVIEWED | Posted: 17 April 2026 doi:10.20944/preprints202604.1260.v1

4.4. Sensor Performance Evaluation Metrics

The performance of sensors was analyzed using three metrics: the Pearson correlation coefficient (r), standard deviation (SD), and mean difference in percentage (MDP) between sensors from non-cumulative measurements. The value of the Pearson correlation coefficient (r) indicates the strength and direction of the relationship between the two variables. Standard deviation (SD) is an essential tool in evaluating PM sensor performance, providing insight into the precision, stability, and overall quality of the sensor's measurements. When a PM sensor repeatedly measures the concentration of PM over a short time frame, the standard deviation of these measurements indicates how much the readings fluctuate. The mean percentage difference (MPD) of sensors refers to the difference in the average readings between two or more sensors that measure the same variable, such as the PM concentration range.

To compare the measurements properly, the data streams must be time-aligned. Due to the difficulty in obtaining data from the PMS5003 sensor at the same intervals for comparison in the experiment results, all sensor time intervals were averaged to 20 seconds, which was defined by the longest sensor data transfer interval. The authors used these averaged data for implementing correction factor models. To accurately assess the performance of the sensor, the authors used non-cumulative measurements for their comparisons. This non-cumulative method allows for the differentiation of PM impacts based on size, as PM1, PM2.5, and PM10 have different effects on human health. Such detailed measurements can aid in the implementation of smart management strategies to reduce pollution and more effectively protect nearby communities. However, using the PMS5003 sensors' non-cumulative measurement approach allows for a more reliable evaluation of size-specific particulate matter data.

4.5. Correction of Non-Cumulative LCPMS Measurements

To improve the accuracy of raw PM measurements from Sniffer4D and PMS5003 in both Standard and Atmospheric modes, size-specific correction factor models were developed by comparing 20sec averaged sensor outputs against a reference (OPC-N3) sensor. Non-cumulative PM measurements averaged into 20-second intervals, were corrected using six modeling techniques: Linear Regression, Second-degree Polynomial Regression, Random Forest (RF), XGBoost (Extreme Gradient Boosting), Artificial Neural Network (ANN), and Kalman Filter. These models were selected based on a literature review highlighting their effectiveness in previous correction studies and their ability to handle both linear and nonlinear sensor response behaviours [28,29,33,37]. Due to the controlled laboratory conditions under which the experiments were conducted, the effects of humidity and temperature were excluded, and each PM size model was trained independently using only the raw sensor readings.

Before applying correction models, the sensor data were time-synchronized with measurements from a reference sensor (OPC-N3), and any invalid or missing values were removed. The dataset for each drilling duration was randomly divided into training (70%) and testing (30%) subsets. To prevent overfitting, 5-fold cross-validation was applied during model development. It provides more stable and reliable estimates of model accuracy by minimizing variance associated with data partitioning, as demonstrated by Hastie et al.(2009) [43]. In this method, the dataset was randomly partitioned into five equal subsets. In each iteration, four folds were used for training and one for validation, rotating through all folds. Hyperparameters for RF and XGBoost were optimized using grid search, while ANN architecture was selected based on validation loss minimization. The ANN model consisted of an input layer (sensor output), two hidden layers (64 and 32 neurons), ReLU activation functions, and a linear output layer. The model was trained using the Adam optimizer with a learning rate of 0.001 for 200 epochs. The performance of each model was evaluated on the test dataset by calculating R^2, RMSE, and MAE, for each PM size fraction and sensor.

© 2026 by the author(s). Distributed under a Creative Commons CC BY license.

Preprints.org (www.preprints.org) | NOT PEER-REVIEWED | Posted: 17 April 2026 doi:10.20944/preprints202604.1260.v1

5. Statistical Results

The statistical results section summarizes the baseline sensor performance measurement and the effectiveness of the applied correction models through quantitative statistical analysis. Subsection 5.1 covers the uncorrected performance of Sniffer4D and PMS5003 sensors using non-cumulative PM measurements at various drilling durations (10, 50, 90 sec), focusing on metrics like correlation (r), standard deviation (SD), and mean percentage difference (MPD). Subsection 5.2 evaluates the performance of correction factor models (Linear, Polynomial, RF, ANN, XGBoost, and Kalman filter) that were applied to sensor data to improve accuracy compared to reference sensor, using statistical indicators such as R^2, RMSE, and MAE.

5.1. Performance Evaluation Analysis from Non-Cumulative Measurements

This section evaluates the raw performance of the Sniffer4D sensor and the PMS5003 sensor Standard and Atmospheric modes across three drilling durations 10, 50, and 90 seconds using non-cumulative PM measurements. It focuses on assessing the correlation of the sensors with the reference sensor, their measurement variability SD, and the degree of measurement bias MPD across PM1, PM2.5, and PM10 particle sizes.

The shortest drilling interval revealed that sensor performance varied significantly across different particle sizes and sensor modes. Figure 4 illustrates sensor readings from a 10-second drilling interval. The Sniffer4D sensor demonstrated moderate correlation for PM1 (r = 0.751, SD = 5 μg/m³, and MPD= 6.38%). However, as shown in Table 2, considerable underestimation was evident for PM2.5 (r = 0.789, SD = 12 μg/m³, MPD = 71.45%) and PM10 (r = 0.785, SD = 20 μg/m³, MPD = -92.115%). The PMS5003 sensor in Standard mode exhibited strong correlations for PM1 (r = 0.886, SD = 19 μg/m³) and PM2.5 (r = 0.848, SD = 45 μg/m³), yet substantial overestimation was observed, notably for PM1 (MPD = 492.05%) and PM2.5 (MPD = 60.466%). PM10 showed moderate correlation (r = 0.706, SD = 96 μg/m³) accompanied by significant underestimation (MPD = -41.241%). In Atmospheric mode, PMS5003 maintained high correlations across all sizes (PM1 r = 0.865, SD = 11 μg/m³; PM2.5 r = 0.854, SD = 29 μg/m³; PM10 r = 0.715, SD = 62 μg/m³), exhibiting lower biases compared to Standard mode, particularly in PM2.5 (MPD = 7.12%). However, PM10 bias remained notably high (MPD = -60.771%).

Increasing the drilling duration to 50 seconds substantially improved sensor performance across all evaluated metrics. Figure 5 highlights sensor readings from 50-sec drilling. Sniffer4D showed significant enhancement in correlations, especially PM1 (r = 0.943, SD = 5 μg/m³, MPD = -11.828%) and PM2.5 (r = 0.925, SD = 11 μg/m³, MPD = -72.71%). PM10 correlation (r = 0.796, SD = 18 μg/m³) improved yet remained lower compared to finer fractions, and bias remained high (MPD = -92.185%).

For PMS5003 Standard mode, correlations were very high (PM1 r = 0.961, SD = 28 μg/m³; PM2.5 r = 0.918, SD = 64 μg/m³; PM10 r = 0.7, SD = 113 μg/m³), yet biases persisted, particularly overestimation in PM1 and PM2.5 (MPD = 451.62% and 69.47%, respectively). Atmospheric mode showed robust correlations (PM1 r = 0.958, SD = 17 μg/m³; PM2.5 r = 0.925, SD = 40 μg/m³; PM10 r = 0.71, SD = 86 μg/m³) with reduced biases relative to Standard mode (PM1 MPD = 268.81%, PM2.5 MPD =13.61%, PM10 MPD = -56.28%).

At the 90-second drilling interval, sensor correlations remained strong yet measurement biases slightly increased. Figure 6 illustrates sensor readings from 90-sec drilling. Sniffer4D consistently yielded high correlation coefficients (PM1 r = 0.903, SD = 5 μg/m³; PM2.5 r = 0.934, SD = 12 μg/m³; PM10 r = 0.855, SD = 20 μg/m³). However, biases increased marginally for PM2.5 (MPD = -77.26%) and PM10 (MPD = -93.71%). PMS5003 Standard mode also produced strong correlations (PM1 r = 0.887, SD = 24 μg/m³; PM2.5 r = 0.88, SD = 65 μg/m³; PM10 r = 0.8, SD = 150 μg/m³) but retained substantial overestimation for fine particles (PM1 MPD = 411.89%, PM2.5 MPD = 46.77%). For PM10, remained underestimation with (MPD = -44.5%). PMS5003 Atmospheric mode correlations remained robust (PM1 r = 0.886, SD = 15 μg/m³; PM2.5 r = 0.882, SD = 43 μg/m³; PM10 r = 0.806, SD = 99 μg/m³),

© 2026 by the author(s). Distributed under a Creative Commons CC BY license.

Preprints.org (www.preprints.org) | NOT PEER-REVIEWED | Posted: 17 April 2026 doi:10.20944/preprints202604.1260.v1

with biases persisting but reduced compared to Standard mode (PM1 MPD = 238.45%, PM2.5 MPD = -2.46%, PM10 MPD = -63.11%).

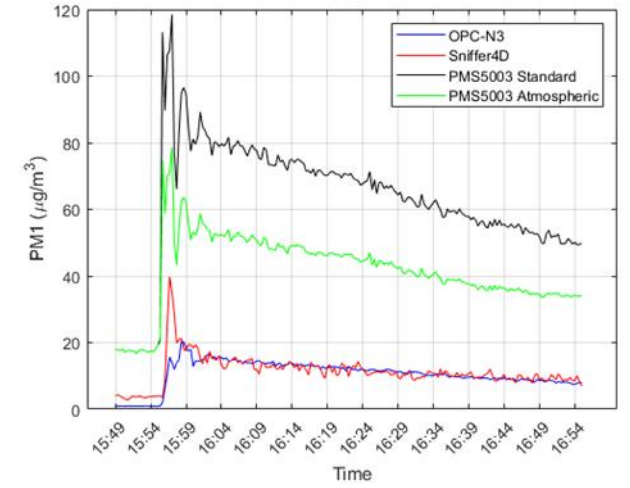

(**a**) PM1

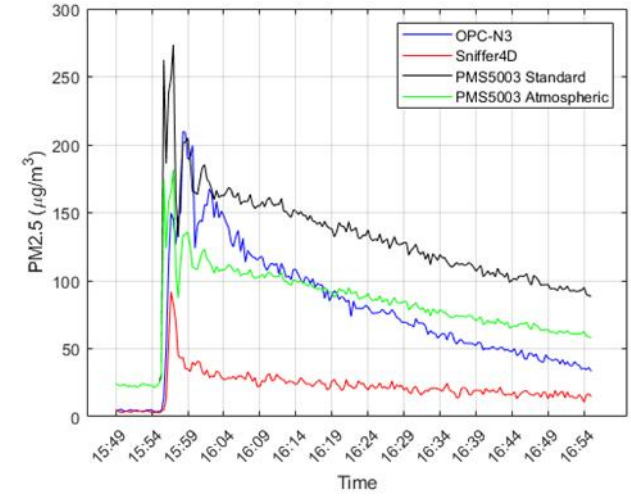

(**b**) PM2.5

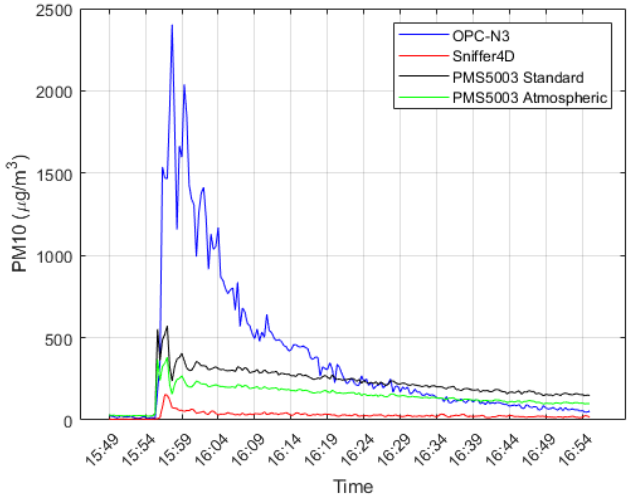

(**c**) PM10

Figure 4. Sensors readings from 10-sec drilling.

© 2026 by the author(s). Distributed under a Creative Commons CC BY license.

Preprints.org (www.preprints.org) | NOT PEER-REVIEWED | Posted: 17 April 2026 doi:10.20944/preprints202604.1260.v1

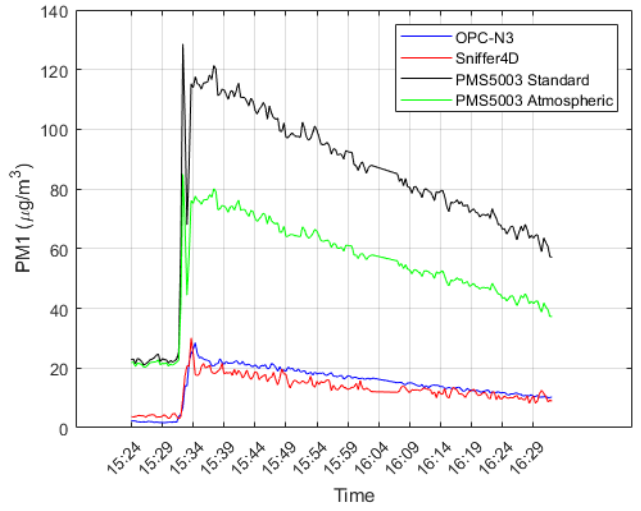

(**a**) PM1

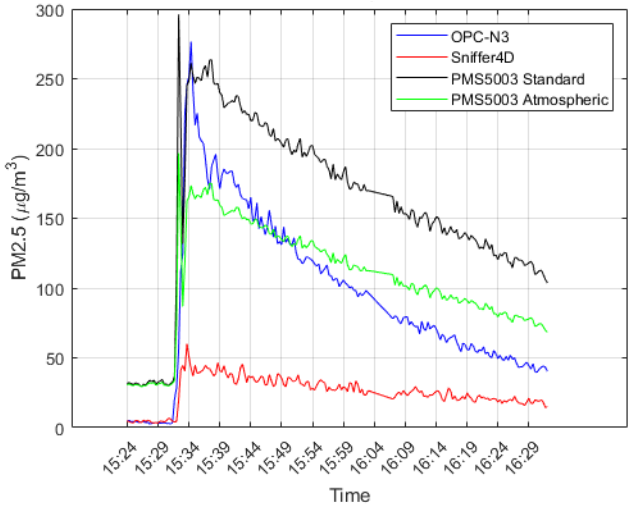

(**b**) PM2.5

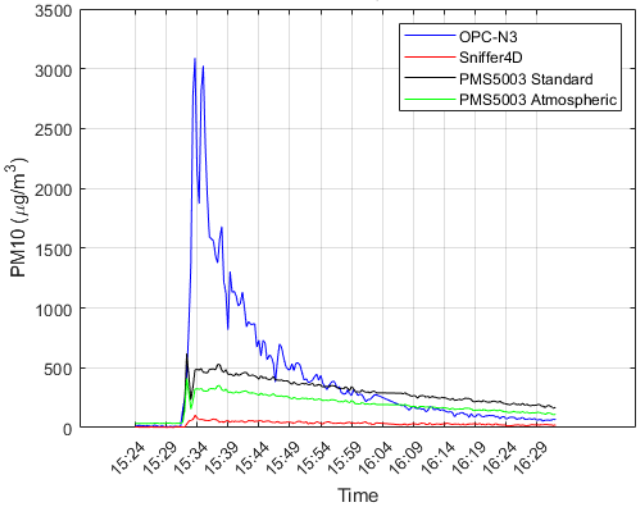

(**c**) PM10

Figure 5. Sensors readings from 50-sec drilling.

© 2026 by the author(s). Distributed under a Creative Commons CC BY license.

Preprints.org (www.preprints.org) | NOT PEER-REVIEWED | Posted: 17 April 2026 doi:10.20944/preprints202604.1260.v1

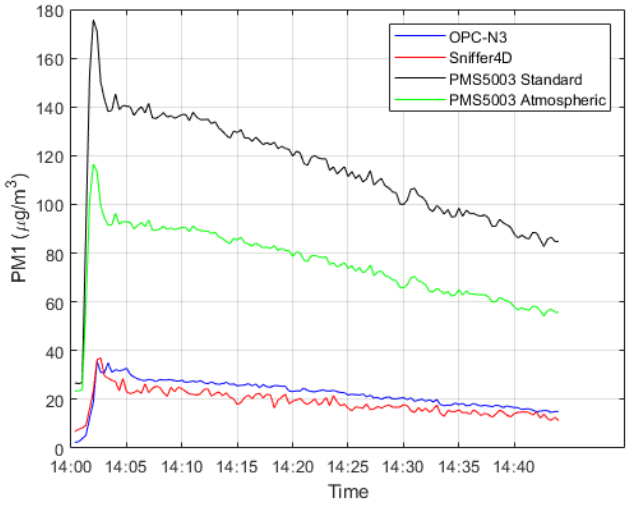

(**a**) PM1

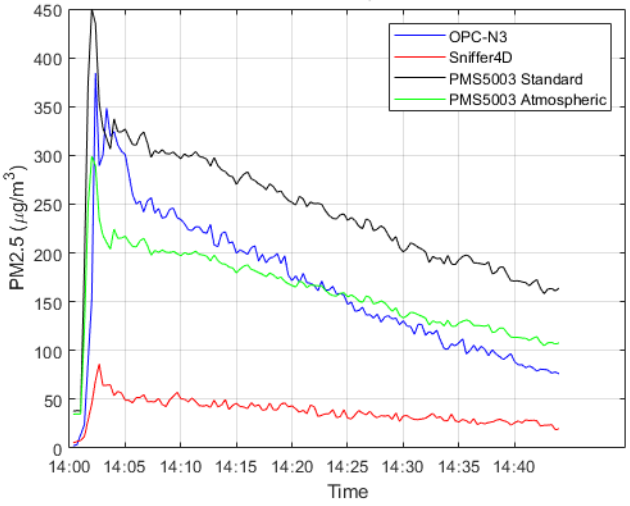

(**b**) PM2.5

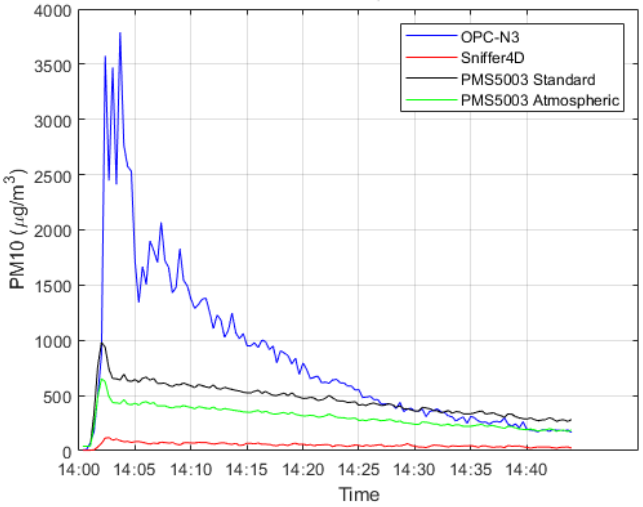

(**c**) PM10

Figure 6. Sensors readings from 90-sec drilling.

Table 2 summarizes the key statistics—including r, SD, and MPD—derived from the non-cumulative PM measurements presented in Figures 4–6. These results highlight how sensor performance changes across particle sizes and drilling durations.

© 2026 by the author(s). Distributed under a Creative Commons CC BY license.

Preprints.org (www.preprints.org) | NOT PEER-REVIEWED | Posted: 17 April 2026 doi:10.20944/preprints202604.1260.v1

Table 2. Statistics from non-cumulative measurements in laboratory experiments.

Laboratory Experiment			Precision and Consistency	Trend recognition	Accuracy
Experiment	**Sensor**	**PM**	**Standard Dev. (SD) (μg/m³)**	**Pearson Corr. (r) with OPC-N3**	**MPD* (%) with OPC-N3**
10-second drilling	Sniffer4D	PM1	5	0.752	6.38
		PM2.5	12	0.789	-71.45
		PM10	20	0.785	-92.115
	PMS5003 Standard	PM1	19	0.886	492.048
		PM2.5	45	0.848	60.466
		PM10	96	0.706	-41.241
	PMS5003 Atmospheric	PM1	11	0.865	295
		PM2.5	29	0.854	7.121
		PM10	62	0.715	-60.771
50-second drilling	Sniffer4D	PM1	5	0.943	-11.828
		PM2.5	11	0.925	-72.71
		PM10	18	0.796	-92.185
	PMS5003 Standard	PM1	28	0.961	451.62
		PM2.5	64	0.918	69.47
		PM10	133	0.7	-34.731
	PMS5003 Atmospheric	PM1	17	0.958	268.81
		PM2.5	40	0.925	13.61
		PM10	86	0.71	-56.283
90-second drilling	Sniffer4D	PM1	5	0.903	-16
		PM2.5	12	0.934	-77.26
		PM10	20	0.855	-93.71
	PMS5003 Standard	PM1	24	0.887	411.89
		PM2.5	65	0.88	46.77
		PM10	150	0.8	-44.5
	PMS5003 Atmospheric	PM1	15	0.886	238.45
		PM2.5	43	0.882	-2.46
		PM10	99	0.806	-63.107

* Mean percentage differences - MPD.

5.2. Evaluation of LCPMS Correction Factor Model Performance

This section evaluates various correction models, including Linear Regression, Polynomial Regression, Random Forest (RF), XGBoost, Artificial Neural Network (ANN), and Kalman Filter, applied to PM1, PM2.5, and PM10 measurements from the Sniffer4D and PMS5003 sensors during different drilling duration. The goal is to assess the accuracy of each model against a reference instrument using metrics such as R^2, RMSE, and MAE, identifying the best models for correcting sensor inaccuracies in dynamic particulate conditions.

For the Sniffer4D sensor at a 10-second drilling interval, the calibration for PM1 initially demonstrated moderate Linear regression performance, with an R^2 value of 0.52, RMSE of 2.8 μg/m³, and MAE of 1.9 μg/m³. However, using Polynomial regression significantly improved the correlation, resulting in an R^2 value of 0.85, an RMSE of 1.6 μg/m³, and an MAE of 1.22 μg/m³. Among various machine learning models, the RF model provided the highest accuracy, achieving an R^2 of 0.87, an RMSE of 1.5 μg/m³, and an MAE ranging from 0.7 to 1.5 μg/m³. The ANN closely followed this, which yielded an R^2 of 0.84 an RMSE of 1.7 μg/m³, and an MAE of 1.23 μg/m³. In contrast, the XGBoost model exhibited lower effectiveness, with an R^2 of only 0.72, while the Kalman filter showed inconsistent results, with an R^2 of 0.72 and an RMSE of 2.2 μg/m³. For PM2.5, Linear regression showcased limited performance with an R^2 of 0.56 and an RMSE of 28.6 μg/m³.

© 2026 by the author(s). Distributed under a Creative Commons CC BY license.

Preprints.org (www.preprints.org) | NOT PEER-REVIEWED | Posted: 17 April 2026 doi:10.20944/preprints202604.1260.v1

However, applying Polynomial regression led to a significant improvement, raising the R^2 to 0.80, lowering the RMSE to 20.1 μg/m³ and MAE to 15.739 μg/m³. Both the ANN and RF models further enhanced the accuracy, reaching an R^2 of 0.87 and an RMSE of 16.5 μg/m³ and MAE 12-13 μg/m³ respectively. PM10 calibration proved challenging due to a low Linear correction, with an R^2 of only 0.57 an RMSE of 284 μg/m³, and with very high MAE of 191.03 μg/m³. Nevertheless, the ANN and RF models yielded notable performance improvements, achieving R^2 values of 0.77 and 0.73, respectively. The Kalman filter continued to show poor performance across all particle sizes.

For the PMS5003 Standard sensor, Linear regression for PM1 at a 10-second drilling interval yielded relatively good performance, with an R^2 of 0.72, RMSE of 1.774 μg/m³, and MAE of 0.922 μg/m³. This performance was slightly improved by Polynomial regression, which resulted in an R^2 of 0.77. The RF model provided the highest accuracy, with an R^2 of 0.87 an RMSE of 1.5 μg/m³, and MAE of 0.67 μg/m³, followed closely by the ANN model. The XGBoost model demonstrated modest performance, achieving an R^2 of 0.73 RMSE of 2.161 μg/m³, and an MAE of 11.434 μg/m³. For PM2.5, the results from linear regression were moderate, with an R^2 of 0.65. However, both RF and ANN models achieved significantly higher correlations, reaching R^2 values between 0.82 and 0.81, with RMSE of 19.19 and 19.69 μg/m³ and MAE of 8.28 and 8.37 μg/m³ respectively. The Polynomial regression model correction for PM10 was notably weakest, with an R^2 of just 0.24, and only modest improvements were observed when using advanced models such as ANN, with a maximum R^2 of 0.63, with RMSE 276.95 μg/m³, and MAE of 121.29 μg/m³.

For the PMS5003 Atmospheric mode operating at a 10-second interval, the Linear regression results for PM1 were comparable to those of the PMS5003 Standard mode. Polynomial regression provided moderate accuracy, achieving an R^2 value of 0.80, RMSE of 1.529 μg/m³, and MAE of 0.87 μg/m³. RF and ANN methods significantly enhanced accuracy, reaching R^2 values between 0.87 and 0.80, with RMSE of 1.492 and1.857 μg/m³, and MAE of 0.658 and 0.773 μg/m³ respectively. For PM2.5, the Linear regression results were moderate, with an R^2 value of 0.65, RMSE of 22.77 μg/m³, and MAE of 13.78 μg/m³. However, RF and ANN models greatly improved accuracy, resulting in R^2 values ranging from 0.82 to 0.81. Conversely, the Linear correction for PM10 was poor, with an R^2 value of only 0.34. Advanced modeling techniques, ANN offered limited improvements, with a maximum R^2 value of 0.63, RMSE of 273.27 μg/m³, and MAE of 110.77 μg/m³. Figure 7 illustrate visual plots of best performed models across PM sizes and sensors from 10-sec drilling. Overall, Table 3 illustrates the performance of correction models from 10-sec drilling and visual plots of best performed models provided in Figure 7, full visual plots provided in Supplementary Figure S1.

For the Sniffer4D sensor using a 50-second drilling interval, Polynomial regression significantly enhanced the calibration of PM1 and PM10 compared to Linear regression. The R^2 value for PM1 increased from 0.86 to 0.92, while for PM10 it improved from 0.63 to 0.73. Additionally, the RMSE was reduced from 2.06 to 1.72 μg/m³ for PM1 and from 345 to 291 μg/m³ for PM10. Among the tested machine learning models, the ANN exhibited the best performance for PM1, achieving an R^2 of 0.922, and for PM10, it reached an R^2 of 0.79 with an RMSE of 263 μg/m³ and MAE of 148 μg/m³. XGBoost demonstrated moderate performance for PM1, with an R^2 of 0.778, which was slightly lower than that of the ANN. Furthermore, it showed little improvement for PM2.5, with an R^2 of 0.711, in comparison to Polynomial regression, which had an R^2 of 0.855.

The PMS5003 Standard mode displayed a strong performance in correcting PM1 levels using linear regression, achieving an R^2 of 0.919, an RMSE of 1.40 μg/m³, and an MAE of 0.772 μg/m³. The RF model yielded the highest accuracy with an R^2 of 0.927, an RMSE of 1.69 μg/m³, and an MAE of 0.8 μg/m³. In comparison, XGBoost had an R^2 of 0.800, and the ANN performed better with an R^2 of 0.921, presenting an RMSE of 1.76 μg/m³. For PM2.5, the RF model again outperformed others, achieving the best overall performance with an R^2 of 0.879, an RMSE of 21.14 μg/m³, and an MAE of 9.4 μg/m³. Polynomial regression followed closely behind, with an R^2 of 0.868 and the lowest RMSE of 18.86 μg/m³. For PM10, polynomial regression demonstrated improved accuracy compared to linear regression, achieving an R^2 of 0.634, an RMSE of 345.05 μg/m³, and an MAE of 163.36 μg/m³. The RF model exhibited slightly lower performance with an R^2 of 0.612, an RMSE of 359.07 μg/m³,

© 2026 by the author(s). Distributed under a Creative Commons CC BY license.

Preprints.org (www.preprints.org) | NOT PEER-REVIEWED | Posted: 17 April 2026 doi:10.20944/preprints202604.1260.v1

and an MAE of 145.17 μg/m³. Overall, the XGBoost model achieved the highest accuracy for PM10 with an R^2 of 0.627, an RMSE of 351.53 μg/m³, and an MAE of 160.43 μg/m³.

Sniffer4d	PMS5003 Standard	PMS5003 Atmospheric
PM1		
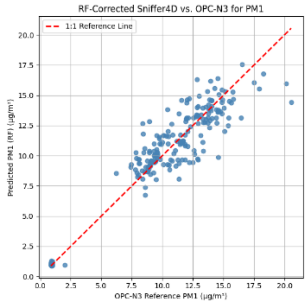	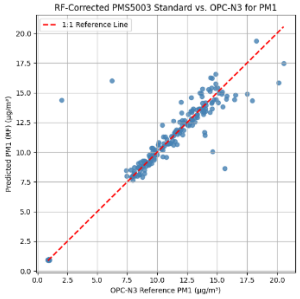	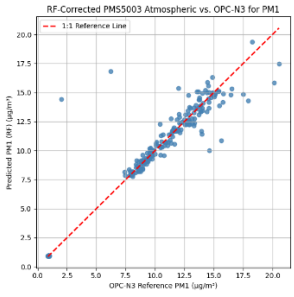
Random Forest	Random Forest	Random Forest
PM2.5		
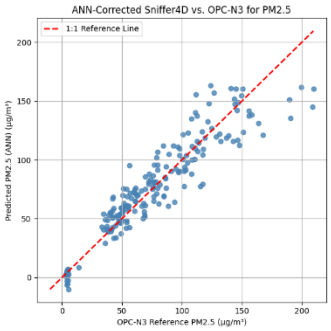	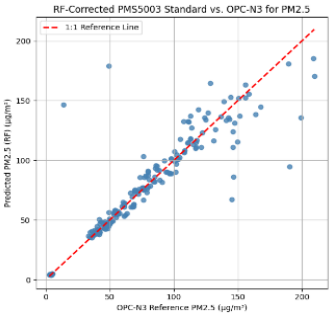	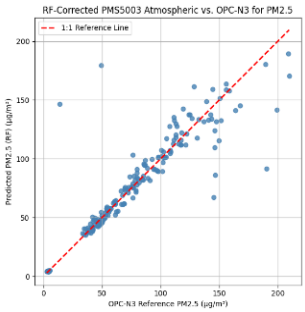
ANN	Random Forest	Random Forest
PM10		
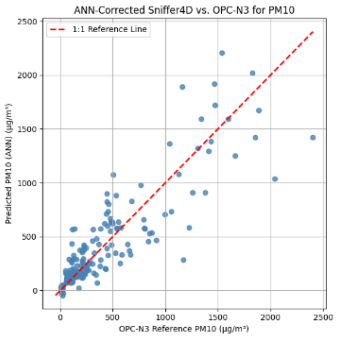	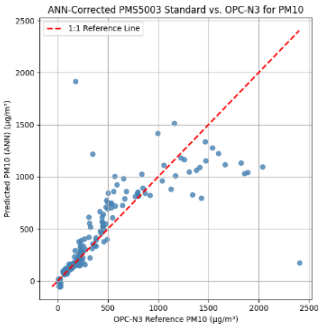	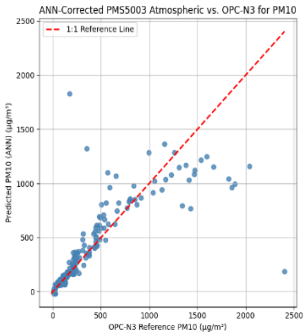
ANN	ANN	ANN

Figure 7. Visual plots of best-performed models across PM sizes and sensors from 10-sec drilling.

Table 3. Statistics from size-specific correction model application from 10 sec drilling.

10-second drilling		Correction Models Name					
Sensor	**Metrics**	**Linear Regression**	**Polynomial degree 2**	**Random Forest**	**XGBoost**	**ANN**	**Kalman Filter**
				PM1			
Sniffer4d	R^2	0.523	0.846	0.86	0.734	0.837	0.72
	RMSE	2.796	1.596	1.542	2.124	1.664	2.18
	MAE	1.933	1.122	1.138	1.676	1.230	1.548

© 2026 by the author(s). Distributed under a Creative Commons CC BY license.

Preprints.org (www.preprints.org) | NOT PEER-REVIEWED | Posted: 17 April 2026 doi:10.20944/preprints202604.1260.v1

PMS5003 Standard	R^2	0.716	0.775	0.866	0.725	0.823	-147.35
	RMSE	1.774	1.636	1.504	2.161	1.731	50.23
	MAE	0.922	0.974	0.67	1.434	0.694	48.409
PMS5003 Atmospheric	R^2	0.669	0.80	0.869	0.718	0.797	-52.55
	RMSE	1.967	1.529	1.492	2.186	1.857	30.18
	MAE	1.073	0.87	0.658	1.463	0.773	29.524
PM2.5							
Sniffer4d	R^2	0.565	0.796	0.844	0.825	0.865	-1.351
	RMSE	28.567	20.052	17.71	18.73	16.46	68.83
	MAE	19.434	15.739	13.06	13.659	12	55.596
PMS5003 Standard	R^2	0.650	0.615	0.817	0.712	0.807	-0.612
	RMSE	23.35	24.39	19.19	24.07	19.69	56.99
	MAE	15.27	16.18	8.28	16.40	8.367	52.36
PMS5003 Atmospheric	R^2	0.652	0.64	0.818	0.715	0.812	0.283
	RMSE	22.77	23.59	19.09	23.94	19.45	38.005
	MAE	13.78	15.51	8.182	16.36	9.308	29.196
PM10							
Sniffer4d	R^2	0.570	0.626	0.734	0.725	0.768	-0.552
	RMSE	283.64	255.29	234.97	239.27	219.6	568.51
	MAE	191.03	195.45	141.54	144.27	136.58	345.14
PMS5003 Standard	R^2	0.338	0.236	0.595	0.533	0.631	-0.112
	RMSE	323.9	324.98	290.27	311.76	276.95	481.21
	MAE	224.57	199.47	117.44	165.84	121.29	259.21
PMS5003 Atmospheric	R^2	0.345	0.245	0.587	0.534	0.641	-0.238
	RMSE	319.89	323.86	292.9	311.29	273.27	507.9
	MAE	217.73	200.02	119.08	165.23	110.77	263.99

* ANN-Artificial Neural Networks; *Polynomial degree 2-Polynomial Regression degree 2; *R^2-Coefficient of Determination; *RMSE- Root Mean Square Error; *MAE- Mean Absolute Error.

In PMS5003 Atmospheric mode, the calibration for PM1 was highly effective using RF, which achieved R^2 of 0.924, RMSE of 1.73 μg/m³, and an MAE of 0.80 μg/m³. ANN also performed well, with an R^2 of 0.919 an RMSE of 1.85 μg/m³, and an MAE of 0.78. Polynomial regression yielded comparable accuracy, with an R^2 of 0.914 and an RMSE of 1.48 μg/m³. PM2.5 results were consistent across Linear, Polynomial regressions and RF models with R^2 0.87-0.88 and RMSE 19-21 μg/m³ and an MAE of 9.3-14.25 μg/m³, with slightly lower ANN performance with R^2=0.85 and the lowest accuracy by XGBoost with R^2 0.7, RMSE 29 μg/m³ and MAE of 21.32 μg/m³. PM10 calibration improved moderately with Polynomial regression with R^2=0.62, and RF and XGBoost provided comparable outcomes. In contrast, the Kalman filter significantly underperformed with negative R^2 values and very high RMSE for all PM sizes and sensors. Figure 8 illustrate visual plots of best performed models across PM sizes and sensors from 50-sec drilling. Detailed performance results are summarized in Table 4, with visual plots provided in Supplementary Figure S2.

At the 90-second interval, the Linear calibration of the Sniffer4D sensor for PM1 showed a lower performance R^2 with 0.77, RMSE of 2.686 μg/m³, and MAE of 1.81 μg/m³ compared to the results obtained at the 50-second drilling. However, using Polynomial regression significantly improved the performance, resulting in an R^2 of 0.86, RMSE of 1.994 μg/m³, and MAE of 1.49 μg/m³. Both RF and ANN demonstrated consistently high accuracy, with R^2 values around 0.87 with RMSE 2.149 μg/m³ for RF and 2.16μg/m³ for ANN and MAE of 1.49 and 1.55 μg/m³ respectively. For PM2.5, the Linear models exhibited strong performance, achieving an R^2 value of approximately 0.86, RMSE 25.984, and 28.411 μg/m³ from Linear Regression and Polynomial respectively, with RF providing slightly better results at R^2 = 0.88 with RMSE 24.649 μg/m³ and MAE of 18.61 μg/m³. The Linear correction for PM10 reached R^2 of approximately 0.63, but this was significantly enhanced by the ANN and RF models, yielding R^2 values between 0.78 and 0.79.

© 2026 by the author(s). Distributed under a Creative Commons CC BY license.

Preprints.org (www.preprints.org) | NOT PEER-REVIEWED | Posted: 17 April 2026 doi:10.20944/preprints202604.1260.v1

Sniffer4d	PMS5003 Standard	PMS5003 Atmospheric
PM1		
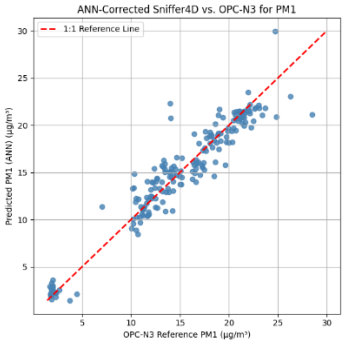	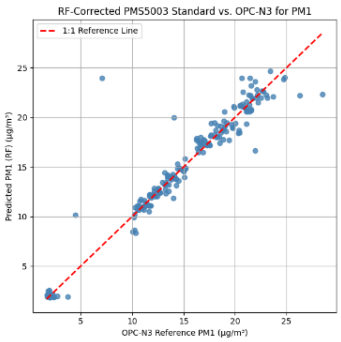	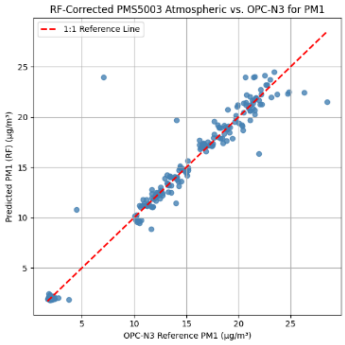
ANN	Random Forest	Random Forest
PM2.5		
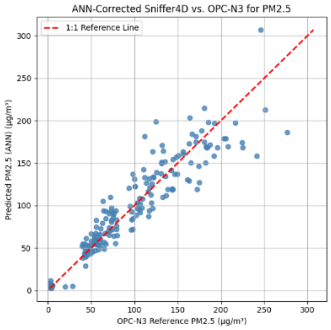	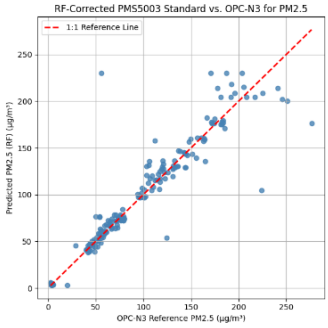	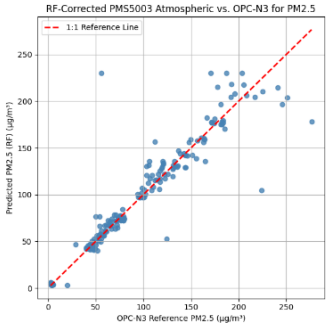
ANN	Random Forest	Random Forest
PM10		
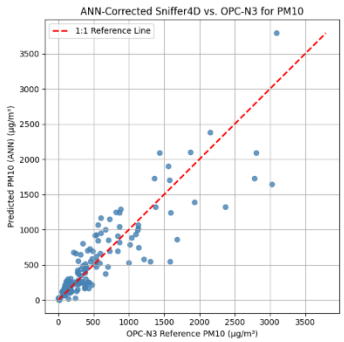	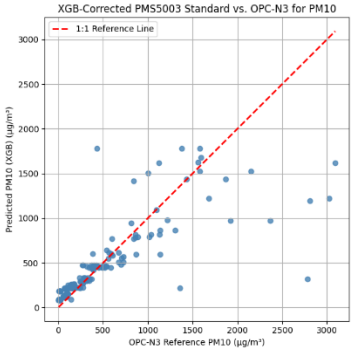	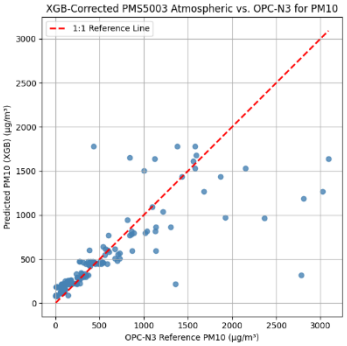
ANN	XGboost	XGboost

Figure 8. Visual plots of best-performed models across PM sizes and sensors from 50-sec drilling.

Table 4. Statistics from size-specific correction model application from 50 sec drilling.

50-second drilling		Correction Models Name					
Sensor	**Metrics**	**Linear Regression**	**Polynomial degree 2**	**Random Forest**	**XGBoost**	**ANN**	**Kalman Filter**
				PM1			
Sniffer4d	R^2	0.886	0.921	0.888	0.778	0.922	0.338
	RMSE	2.061	1.718	2.091	2.944	1.744	5.080
	MAE	1.511	1.251	1.431	2.401	1.216	3.222
PMS5003 Standard	R^2	0.919	0.911	0.927	0.800	0.921	-102.06
	RMSE	1.402	1.475	1.693	2.796	1.759	63.402
	MAE	0.772	0.813	0.800	2.096	0.748	59.940
PMS5003 Atmospheric	R^2	0.910	0.914	0.924	0.802	0.919	-35.600
	RMSE	1.503	1.476	1.727	2.781	1.776	37.782
	MAE	0.866	0.816	0.803	2.087	0.778	36.242

© 2026 by the author(s). Distributed under a Creative Commons CC BY license.

Preprints.org (www.preprints.org) | NOT PEER-REVIEWED | Posted: 17 April 2026 doi:10.20944/preprints202604.1260.v1

PM2.5							
Sniffer4d	R^2	0.852	0.855	0.838	0.711	0.876	-1.196
	RMSE	22.964	22.608	24.511	32.715	21.387	90.149
	MAE	17.971	15.954	16.441	25.125	14.658	69.747
PMS5003 Standard	R^2	0.849	0.868	0.879	0.778	0.864	-0.804
	RMSE	22.642	18.858	21.141	28.660	22.437	81.701
	MAE	16.565	9.785	9.403	21.401	9.287	73.634
PMS5003 Atmospheric	R^2	0.868	0.868	0.880	0.778	0.850	0.187
	RMSE	20.790	18.951	21.065	28.686	23.581	54.836
	MAE	14.252	9.922	9.315	21.324	9.126	43.023
PM10							
Sniffer4d	R^2	0.627	0.730	0.782	0.730	0.793	-0.471
	RMSE	344.938	291.071	269.835	300.285	263.123	700.856
	MAE	254.723	163.971	153.877	158.749	148.008	398.259
PMS5003 Standard	R^2	0.486	0.625	0.613	0.630	0.439	-0.111
	RMSE	404.078	345.227	359.409	351.539	432.856	608.992
	MAE	274.451	163.356	145.165	160.430	152.689	317.188
PMS5003 Atmospheric	R^2	0.503	0.622	0.618	0.629	0.531	-0.196
	RMSE	397.556	346.439	357.370	352.195	395.706	631.894
	MAE	265.713	163.440	144.327	160.763	142.142	314.844

* ANN-Artificial Neural Networks; *Polynomial degree 2-Polynomial Regression degree 2; *R^2-Coefficient of Determination; *RMSE- Root Mean Square Error; *MAE- Mean Absolute Error.

In the case of PMS5003 Standard at 90 seconds, the Linear correction results for PM1 remained moderate, achieving an R^2 of about 0.76, RMSE of 2.41 μg/m³, and MAE of 1.17 μg/m³. Both RF and ANN slightly outperformed the Linear models, with R^2 values around 0.82, RMSE of 2.6 μg/m³, and MAE of 1.17 and 1.11 μg/m³ respectively. The Linear correction for PM2.5 was moderate, with R^2 values between 0.77 and 0.78, while RF and ANN provided substantial improvements, resulting in R^2 values of approximately 0.82 to 0.83 with RMSE of 30.66 and 29.81μg/m³, and MAE of 15.6 and 14.11 μg/m³ respectively. PM10 showed marked improvement from earlier intervals, with a Linear model's R^2 between 0.65 and 0.66, and RF notably enhanced its performance, achieving an R^2 of about 0.73, RMSE of 382.92 μg/m³ and MAE of 175.2 μg/m³.

The performance of the PMS5003 Atmospheric mode at the 90-second interval closely mirrored that of the PMS5003 Standard mode. The linear models for PM1 and PM2.5 performed well, yielding R^2 values of approximately 0.76 and between 0.77 and 0.78, respectively. RF and ANN provided significant enhancements, with PM1 achieving an R^2 of around 0.82, with RMSE of 2.52 and 2.57 μg/m³, and MAE of 1.16 and 1.15 μg/m³ respectively. For PM2.5, RF and ANN reached R^2 0.82 and 0.85, RMSE of 31 and 29 μg/m³, and MAE of 15.92 and 13μg/m³ respectively showing the highest performance accuracy. The correction for PM10 saw considerable improvement, with a linear regression R^2 value between 0.65 and 0.66, which was notably enhanced by the ANN and RF models, achieving R^2 values ranging from 0.74 to 0.78. Figure 9 illustrate visual plots of best performed models across PM sizes and sensors from 90-sec drilling. Detailed performance results are summarized in Table 5, with full visual plots provided in Supplementary Figure S3.

Table 5. Statistics from size-specific correction model application from 90 sec drilling.

90-second drilling		**Correction Models Name**					
Sensor	**Metrics**	**Linear Regression**	**Polynomial degree 2**	**Random Forest**	**XGBoost**	**ANN**	**Kalman Filter**
PM1							
Sniffer4d	R^2	0.769	0.857	0.868	0.711	0.866	0.462
	RMSE	2.686	1.994	2.149	3.175	2.162	4.336
	MAE	1.807	1.488	1.485	2.399	1.551	2.994

© 2026 by the author(s). Distributed under a Creative Commons CC BY license.

Preprints.org (www.preprints.org) | NOT PEER-REVIEWED | Posted: 17 April 2026 doi:10.20944/preprints202604.1260.v1

PMS5003 Standard	R^2	0.762	0.747	0.814	0.634	0.819	-258.21
	RMSE	2.408	2.650	2.547	3.575	2.516	95.146
	MAE	1.166	1.332	1.169	2.243	1.110	93.942
PMS5003 Atmospheric	R^2	0.757	0.763	0.818	0.632	0.811	-87.501
	RMSE	2.441	2.558	2.523	3.583	2.568	55.595
	MAE	1.175	1.296	1.158	2.252	1.148	55.012
PM2.5							
Sniffer4d	R^2	0.856	0.826	0.884	0.819	0.861	-2.857
	RMSE	25.984	28.411	24.649	30.837	26.976	142.325
	MAE	19.681	20.827	18.613	23.281	19.122	125.686
PMS5003 Standard	R^2	0.770	0.708	0.821	0.659	0.831	-0.964
	RMSE	31.997	37.047	30.655	42.294	29.811	101.563
	MAE	17.510	19.024	15.600	26.989	14.118	95.977
PMS5003 Atmospheric	R^2	0.775	0.725	0.817	0.657	0.845	0.444
	RMSE	31.393	35.895	30.977	42.443	28.500	54.052
	MAE	16.577	18.282	15.923	27.051	13.508	41.974
PM10							
Sniffer4d	R^2	0.631	0.716	0.769	0.722	0.782	-1.089
	RMSE	382.981	352.373	352.220	386.560	342.244	1059.139
	MAE	282.104	245.482	246.894	258.529	226.507	770.193
PMS5003 Standard	R^2	0.648	0.572	0.727	0.636	0.240	-0.079
	RMSE	408.602	456.303	382.917	441.939	638.913	761.281
	MAE	249.683	246.940	175.201	192.476	208.191	451.288
PMS5003 Atmospheric	R^2	0.662	0.557	0.738	0.607	0.785	-0.371
	RMSE	400.841	462.793	375.085	459.560	340.057	858.092
	MAE	245.589	250.178	173.387	199.880	156.984	518.291

* ANN-Artificial Neural Networks; *Polynomial degree 2-Polynomial Regression degree 2; *R^2-Coefficient of Determination; *RMSE- Root Mean Square Error; *MAE- Mean Absolute Error.

Sniffer4d	**PMS5003 Standard**	**PMS5003 Atmospheric**
PM1		
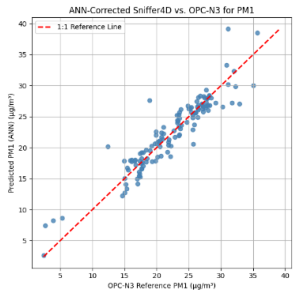	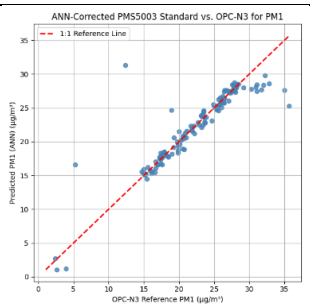	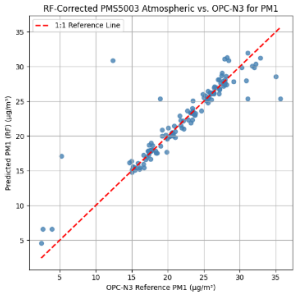
ANN	ANN	Random Forest
PM2.5		
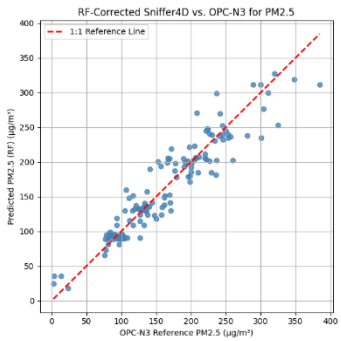	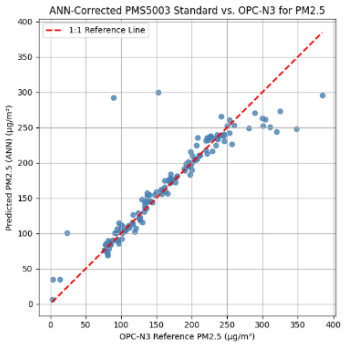	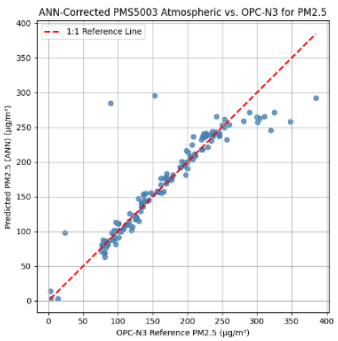
Random Forest	ANN	ANN
PM10		

© 2026 by the author(s). Distributed under a Creative Commons CC BY license.

Preprints.org (www.preprints.org) | NOT PEER-REVIEWED | Posted: 17 April 2026 doi:10.20944/preprints202604.1260.v1

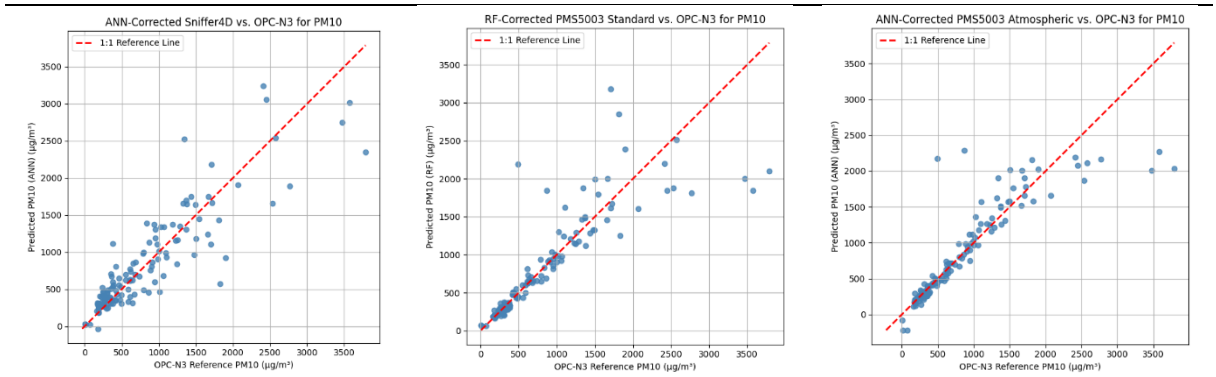

ANN | Random Forest | ANN

Figure 9. Visual plots of best-performed models across PM sizes and sensors from 90-sec drilling.

6. Discussion

6.1. Performance Evaluation

This study critically evaluated the limitations and accuracy constraints of low-cost PM sensors—Sniffer4D and PMS5003 Standard and Atmospheric modes—in measuring PM concentrations generated from construction-related activities.

Sensor limitations were particularly pronounced at the shortest 10-second drilling. Sniffer4D exhibited only moderate correlations, with substantial overestimations for PM2.5 and PM10, reflecting its limited capacity to accurately capture transient, high-intensity particulate emissions characteristic of construction activities. PMS5003 demonstrated markedly different performance depending on operational mode; Standard mode consistently showed significant negative biases in finer particles and positive biases in larger particles, indicating fundamental algorithmic limitations. Conversely, the Atmospheric mode provided relatively better accuracy for fine particulate fractions yet continued to demonstrate notable biases, particularly in PM10, suggesting intrinsic sensor calibration limitations.

At the 50-second drilling, despite observable improvements in sensor correlations and variability, persistent and substantial biases remained, especially notable in PM2.5 and PM10 measurements. The persistence of these biases across both sensors indicates fundamental limitations in sensor technologies, calibration methods, or internal correction algorithms, rather than merely duration-dependent performance improvements. Particularly, the PMS5003 Atmospheric mode consistently showed lower bias compared to the Standard mode, highlighting the importance of sensor internal processing methods in determining accuracy outcomes.

At the longest (90-second) drilling, sensor performance remained hindered by bias increases, particularly evident in coarse particle measurements. This increased bias is likely attributable to sensor drift or saturation. Despite robust correlations across all particle fractions and sensor modes, the persistent biases significantly limit the applicability of these sensors for accurate, quantitative measurements in construction environments, particularly for health-related assessments or regulatory compliance monitoring.

In summary, these findings reveal substantial limitations in current sensor technologies, indicating that low-cost sensors require significant calibration and correction efforts to provide reliable, quantitative data before construction site deployment. The notable disparities in performance between sensor modes further highlight the importance of careful sensor selection and configuration for field applications.

6.2. LCPMS Correction Factor Model Performance

At the shortest 10-sec drilling, the rapid fluctuation in dust emissions introduced considerable measurement instability, placing high demands on model adaptability. For PM1, all three sensors

© 2026 by the author(s). Distributed under a Creative Commons CC BY license.

Preprints.org (www.preprints.org) | NOT PEER-REVIEWED | Posted: 17 April 2026 doi:10.20944/preprints202604.1260.v1

responded best to non-linear and ensemble learning methods. The Sniffer4D sensor particularly benefited from RF and Polynomial regression, both of which captured the short-term variability better than Linear regression, which failed to resolve finer-scale fluctuations. ANN also provided stable performance, although slightly less consistent than RF. PMS5003 Standard and Atmospheric modes showed similar trends, with RF leading in accuracy, while Polynomial and XGBoost regression offered only moderate improvements. Kalman filtering was consistently ineffective, unable to adjust for abrupt concentration changes across all sensors and particle sizes.

For PM2.5, similar model hierarchies were observed. Sniffer4D calibration again favoured ANN and RF, which substantially improved estimation accuracy over XGBoost, Linear, and Polynomial methods. PMS5003Standard and Atmospheric modes also showed clear gains using these models, although the differences between Polynomial and advanced machine learning methods were more pronounced for PM2.5 than for PM1. In contrast, PM10 correction remained difficult across all sensors. Sniffer4D exhibited the most substantial gains when using ANN and RF, but the PMS5003 sensor demonstrated only marginal improvements regardless of the correction approach. These findings indicate that, for brief and dynamic exposure events, model complexity is crucial—particularly for coarse particles, where simpler methods fail to accommodate sensor limitations and environmental noise.

With increased drilling duration, sensor signals became more stable, allowing more consistent calibration across particle sizes and sensors. For PM1, both sensors showed improved performance, with ANN emerging as the most effective model for Sniffer4D, while RF, XGBoost, and Polynomial regression closely followed. In PMS5003 Standard and Atmospheric modes, Linear regression became more viable, but machine learning models still provided the highest reliability and precision. Polynomial regression proved particularly valuable, capturing the modest non-linearity in the sensor–reference relationship without overfitting.

PM2.5 correction at 50 seconds exhibited high model agreement across all approaches. ANN, RF, and XGBoost maintained strong performance for Sniffer4D and PMS5003sensors, while Polynomial regression offered competitive results, suggesting a smoother, more predictable sensor response under intermediate drilling durations. Linear Regression model improved significantly compared to the 10-second case, especially for PMS5003Standard and Atmospheric, but generally trailed behind non-linear techniques. XGBoost, while stable, rarely outperformed ANN or RF.

Despite some improvement, PM10 continued to show greater modeling difficulty. The Sniffer4D sensor retained its relative advantage, especially when corrected with ANN, which captured the variability of coarse particle dispersion more effectively than other methods. PMS5003 sensor both modes, however, remained limited in their correction potential. Even advanced models like XGBoost and RF delivered only modest accuracy, and ANN showed signs of underperformance, possibly due to overfitting to high-magnitude outliers. Across all cases, the Kalman filter remained the least effective approach, with error metrics far exceeding acceptable thresholds, confirming its unsuitability for conditions with dynamic concentration changes.

From a 90-second drilling duration, for PM1 RF and ANN again yielded the most accurate corrections for all sensors, though the performance gap between advanced and simpler models narrowed. Polynomial regression performed well and, in some cases, nearly matched machine learning models, especially for PMS5003 Standard and Atmospheric modes. Linear regression, while not the top performer, produced acceptable results due to the improved signal-to-noise ratio provided by longer averaging.

PM2.5 calibration further validated the benefits of model simplicity under stable conditions. All sensors achieved strong agreement with reference values using Polynomial and Linear models, although RF and ANN consistently maintained a slight edge in accuracy. PMS5003 Atmospheric mode responded well to these models, indicating reduced bias and improved generalizability. These results support the idea that model choice becomes less critical at longer drilling durations, if particle dynamics are less erratic.

© 2026 by the author(s). Distributed under a Creative Commons CC BY license.

Preprints.org (www.preprints.org) | NOT PEER-REVIEWED | Posted: 17 April 2026 doi:10.20944/preprints202604.1260.v1

PM10, while showing some of the most notable gains at 90 seconds, still posed calibration challenges. Sniffer4D maintained better correction accuracy than the PMS5003 sensor, particularly with ANN and RF. For PMS5003 Standard and Atmospheric modes, Polynomial regression contributed the most improvement, while ANN and XGBoost provided only modest additional benefits. Despite the extended drilling period, coarse particle measurement remained affected by sensor limitations and environmental variability. The Kalman filter again failed to track coarse particle trends, reinforcing the need for correction models that can account for both bias and transient concentration surges.

Across all drilling durations, RF and ANN consistently provided the most accurate corrections for both sensors—Sniffer4D, PMS5003 Standard, and PMS5003 Atmospheric modes. For PM1, RF was the best performer at short durations, while ANN led slightly at 50 seconds for Sniffer4D. For PM2.5, both models were highly effective, with RF showing better stability across durations. PM10 calibration, by contrast, revealed fundamental challenges in coarse particle measurement using low-cost optical sensors. Even the best-performing ANN and RF remained the only models to yield acceptable accuracy, particularly for Sniffer4D. Polynomial regression was especially useful for PMS5003 Standard and Atmospheric modes at intermediate drilling durations. Overall, the findings highlight that model selection should be tailored to sensor type and PM size, with RF and ANN emerging as the most robust correction models across dynamic construction dust conditions.

6.3. Comparison with Reported Error Ranges in Previous Studies

The performance trends observed in the present study are consistent with findings reported in prior laboratory and field evaluations of low-cost optical particulate matter sensors. Several studies have documented that, when calibrated against reference-grade instruments, low-cost sensors typically achieve strong agreement for fine particle fractions under ambient conditions. For example, field and laboratory assessments of PMS5003 and OPC-N series sensors have reported coefficients of determination (R^2) generally ranging between 0.70 and 0.95 for PM2.5, depending on aerosol composition and environmental stability [13,14,17,28,33]. Tryner et al. [17] and Kaur and Kelly [14,21] demonstrated high correlations between optical sensors and reference monitors under controlled conditions, while Si et al. [28] and Raheja et al. [33] reported substantial improvement in PM2.5 accuracy following machine-learning-based calibration.

In the present study, corrected PM1 and PM2.5 measurements achieved R^2 values up to 0.92 and 0.88, respectively, under 50- and 90-second drilling intervals. These results fall within the upper range of performance reported in the literature for fine particle calibration, despite the more demanding emission conditions associated with construction dust. This indicates that size-specific correction can achieve accuracy comparable to that observed in ambient monitoring environments.

In contrast, coarse particle (PM10) measurement has consistently shown larger uncertainty in previous investigations. Laboratory evaluations have demonstrated reduced size-selective accuracy for particles larger than 2.5 μm due to optical detection constraints [15,42]. Field studies during dust events have reported moderate correlations for PM10, with R^2 values commonly between 0.50 and 0.85 and substantially higher absolute errors compared to PM2.5 [14,21,36]. Molina Rueda et al. [36] specifically reported greater variability in coarse particle channels relative to fine fractions, highlighting instability in size-resolved performance.

Consistent with these findings, the present study achieved PM10 correction R^2 values up to approximately 0.78 under the 90-second drilling condition. However, absolute error metrics remained considerably higher than those observed for PM1 and PM2.5, particularly under short-duration, high-intensity emission scenarios. This behaviour aligns with previously documented limitations of optical sensors in coarse-dominated aerosol environments [14,15,21].

It is important to note that most prior calibration studies have focused primarily on PM2.5 under relatively stable ambient urban conditions [13,17,28,33]. By contrast, the present investigation evaluates transient, high-concentration construction-generated emissions characterized by rapid concentration fluctuations and a substantial coarse particle component. The comparatively larger

© 2026 by the author(s). Distributed under a Creative Commons CC BY license.

Preprints.org (www.preprints.org) | NOT PEER-REVIEWED | Posted: 17 April 2026 doi:10.20944/preprints202604.1260.v1

PM10 errors observed here therefore reflect not only intrinsic optical sensing constraints but also the extreme and dynamic emission conditions examined.

6.4. Limitations and Future Recommendations

Despite the comprehensive evaluation presented in this study, several limitations should be acknowledged. First, the study was based on short-term laboratory tests, which do not capture the long-term durability and performance of low-cost PM sensors under real-world construction site conditions. Second, the experiments were conducted in a controlled laboratory environment using drilling-induced dust emissions. While this approach ensured repeatability and experimental control, it may not fully replicate the spatial and temporal variability of airborne PM typically observed in dynamic outdoor construction settings. Third, the correction models developed in this study did not incorporate environmental covariates such as relative humidity, temperature, or air turbulence, despite their known influence on PM sensor performance. Integrating these parameters in future model development—especially using multi-variate approaches—could enhance model generalizability and robustness across different environmental contexts.

Future work should aim to validate the proposed correction framework through long-term field deployments in active construction sites and expand model inputs to account for meteorological variables. Such advancements would further support the deployment of reliable, low-cost PM monitoring systems tailored for urban sustainability and occupational health management.

7. Conclusions

This study presents a comprehensive evaluation of LCPMS under laboratory conditions simulating construction-generated emissions, with a focus on non-cumulative measurements of PM1, PM2.5, and PM10. Unlike typical cumulative reporting, the use of size-resolved data enabled a more accurate assessment of sensor response and health-relevant exposure differentiation—critical for environments where particle composition and dynamics vary significantly.

The evaluation revealed clear differences in sensor performance across PM size fractions. The Sniffer4D sensor showed moderate correlations with the reference (OPC-N3) for PM1 and PM2.5 but substantially overestimated PM10 levels. In contrast, the PMS5003 sensor in Atmospheric mode demonstrated improved correlation and reduced variability for fine particles, although significant negative bias persisted—especially for PM10. Standard deviation and mean percentage difference (MPD) metrics confirmed that raw sensor outputs, particularly for PM10, are not directly suitable for precise monitoring without correction.

To address these limitations, six correction models—Linear Regression, Polynomial Regression, Random Forest (RF), XGBoost, Artificial Neural Network (ANN), and Kalman Filter—were developed and evaluated independently for each PM size and drilling duration. Results showed that RF and ANN consistently provided the most accurate corrections across PM1, PM2.5, and PM10. For PM1, Random Forest achieved R^2 values up to 0.87–0.89 across durations. PM2.5 corrections were similarly effective, with ANN and RF reaching $R^2 = 0.88$. PM10 was the most difficult to correct, but ANN still reached $R^2 = 0.79$ for Sniffer4D. In contrast, the Kalman Filter consistently underperformed across all size fractions and sensors, indicating its limited applicability under dynamic, high-dust conditions.

These findings confirm that correction model performance is PM size–specific and strongly influenced by activity duration. Importantly, the effectiveness of RF and ANN in capturing real-time PM variability supports their integration into sensor networks for regulatory monitoring, exposure assessment, and smart city applications. The findings reaffirm that no universal correction factor can accommodate the unique characteristics of PM1, PM2.5, and PM10. Thus, adopting PM size–specific correction approaches is crucial for ensuring data quality and protecting public health in dust-intensive urban environments. This highlights the need for dedicated, particle–size–specific calibration strategies when deploying low-cost sensors in complex environments, such as construction sites.

© 2026 by the author(s). Distributed under a Creative Commons CC BY license.

Preprints.org (www.preprints.org) | NOT PEER-REVIEWED | Posted: 17 April 2026 doi:10.20944/preprints202604.1260.v1

This study recommends to sensor developers and the scientific community that future monitoring systems prioritize non-cumulative data reporting and support independent correction modeling for each PM fraction. Doing so will ensure more accurate exposure assessments, enable responsive dust control strategies, and promote sustainable, health-conscious urban development.

Supplementary Materials: The following supporting information can be downloaded at the website of this paper posted on Preprints.org, Table S1: Overview of previous LCPMS evaluation and calibration studies; Figure S1: Correction factor plots from 10-second drilling; Figure S2: Correction factor plots from 50-second drilling; Figure S3: Correction factor plots from 90-second drilling.

Author Contributions: Askarov Komiljon: Writing – review & editing, Writing – original draft, Visualization, Methodology, Investigation, Formal analysis, Data curation, Conceptualization. **Jae-ho Choi:** Writing – review & editing, Supervision, Funding acquisition, Methodology, Conceptualization.

Data Availability Statement: Row data and analyzed data used in this study are available upon request.

Acknowledgments: This work was supported and funded by the National Foundation of Korea (NRF) grant funded by the Korea government (MSIT) (RS-2026-25488534).

Conflicts of Interest: The authors declare that they have no known competing financial interests or personal relationships that could have appeared to influence the work reported in this paper.:.

Abbreviations

The following abbreviations are used in this manuscript:

ANN	Artificial Neural Network
BAM	Beta Attenuation Monitor
CV	Coefficient of Variation
EIA	Environmental Impact Assessment
FEM	Federal Equivalent Method
FRM	Federal Reference Method
IoT	Internet of Things
LCPMS	Low-Cost Particulate Matter Sensors
MAE	Mean Absolute Error
MPD	Mean Percentage Difference
MSE	Mean Squared Error
PM	Particulate Matter
PM1	Particulate Matter with aerodynamic diameter ≤ 1 μm
PM2.5	Particulate Matter with aerodynamic diameter ≤ 2.5 μm
PM10	Particulate Matter with aerodynamic diameter ≤ 10 μm
RF	Random Forest
RMSE	Root Mean Square Error
R^2	Coefficient of Determination
SD	Standard Deviation
TSI	Tapered Element Oscillating Microbalance Manufacturer (TSI Incorporated)
USEPA	United States Environmental Protection Agency
WHO	World Health Organization
XGBoost	Extreme Gradient Boosting

References

1. Marsh, D.; Green, D. *Air Quality and Emissions in Construction*; 2022;
2. Yang, J.; Tae, S.; Kim, H. Technology for Predicting Particulate Matter Emissions at Construction Sites in South Korea. *Sustainability* **2021**, *13*, doi:10.3390/su132413792.
3. WHO WHO Global Air Quality Guidelines: Particulate Matter (PM2.5 and PM10), Ozone, Nitrogen Dioxide, Sulfur Dioxide and Carbon Monoxide Available online: https://www.who.int/publications/i/item/9789240034228 (accessed on 12 February 2026).

© 2026 by the author(s). Distributed under a Creative Commons CC BY license.

Preprints.org (www.preprints.org) | NOT PEER-REVIEWED | Posted: 17 April 2026 doi:10.20944/preprints202604.1260.v1

4. Apte, J.S.; Brauer, M.; Cohen, A.J.; Ezzati, M.; Pope, C.A.I. Ambient PM2.5 Reduces Global and Regional Life Expectancy. *Environ. Sci. Technol. Lett.* **2018**, *5*, 546–551, doi:10.1021/acs.estlett.8b00360.
5. Khamraev, K.; Cheriyan, D.; Choi, J. A Review on Health Risk Assessment of PM in the Construction Industry – Current Situation and Future Directions. *Sci. Total Environ.* **2021**, *758*, 143716, doi:10.1016/j.scitotenv.2020.143716.
6. EU EU Air Quality Standards - Environment - European Commission Available online: https://environment.ec.europa.eu/topics/air/air-quality/eu-air-quality-standards_en (accessed on 12 February 2026).
7. USEPA Document Display | NEPIS | US EPA Available online: https://nepis.epa.gov/ (accessed on 12 February 2026).
8. Khan, M.; Khan, N.; Skibniewski, M.J.; Park, C. Environmental Particulate Matter (PM) Exposure Assessment of Construction Activities Using Low-Cost PM Sensor and Latin Hypercubic Technique. *Sustainability* **2021**, *13*, doi:10.3390/su13147797.
9. Cheriyan, D.; Hyun, K.Y.; Jaegoo, H.; Choi, J. Assessing the Distributional Characteristics of PM10, PM2.5, and PM1 Exposure Profile Produced and Propagated from a Construction Activity. *J. Clean. Prod.* **2020**, *276*, 124335, doi:10.1016/j.jclepro.2020.124335.
10. Steinle, S.; Reis, S.; Sabel, C.E. Quantifying Human Exposure to Air Pollution—Moving from Static Monitoring to Spatio-Temporally Resolved Personal Exposure Assessment. *Sci. Total Environ.* **2013**, *443*, 184–193, doi:10.1016/j.scitotenv.2012.10.098.
11. Castell, N.; Dauge, F.R.; Schneider, P.; Vogt, M.; Lerner, U.; Fishbain, B.; Broday, D.; Bartonova, A. Can Commercial Low-Cost Sensor Platforms Contribute to Air Quality Monitoring and Exposure Estimates? *Environ. Int.* **2017**, *99*, 293–302, doi:10.1016/j.envint.2016.12.007.
12. Morawska, L.; Thai, P.K.; Liu, X.; Asumadu-Sakyi, A.; Ayoko, G.; Bartonova, A.; Bedini, A.; Chai, F.; Christensen, B.; Dunbabin, M.; et al. Applications of Low-Cost Sensing Technologies for Air Quality Monitoring and Exposure Assessment: How Far Have They Gone? *Environ. Int.* **2018**, *116*, 286–299, doi:10.1016/j.envint.2018.04.018.
13. Cowell, N.; Chapman, L.; Bloss, W.; Pope, F. Field Calibration and Evaluation of an Internet-of-Things-Based Particulate Matter Sensor. *Front. Environ. Sci.* **2022**, *9*, doi:10.3389/fenvs.2021.798485.
14. Kaur, K.; Kelly, K.E. Laboratory Evaluation of the Alphasense OPC-N3, and the Plantower PMS5003 and PMS6003 Sensors. *J. Aerosol Sci.* **2023**, *171*, 106181, doi:10.1016/j.jaerosci.2023.106181.
15. Kuula, J.; Mäkelä, T.; Aurela, M.; Teinilä, K.; Varjonen, S.; González, Ó.; Timonen, H. Laboratory Evaluation of Particle-Size Selectivity of Optical Low-Cost Particulate Matter Sensors. *Atmospheric Meas. Tech.* **2020**, *13*, 2413–2423, doi:10.5194/amt-13-2413-2020.
16. Jayaratne, R.; Liu, X.; Thai, P.; Dunbabin, M.; Morawska, L. The Influence of Humidity on the Performance of a Low-Cost Air Particle Mass Sensor and the Effect of Atmospheric Fog. *Atmospheric Meas. Tech.* **2018**, *11*, 4883–4890, doi:10.5194/amt-11-4883-2018.
17. Tryner, J.; L'Orange, C.; Mehaffy, J.; Miller-Lionberg, D.; Hofstetter, J.C.; Wilson, A.; Volckens, J. Laboratory Evaluation of Low-Cost PurpleAir PM Monitors and in-Field Correction Using Co-Located Portable Filter Samplers. *Atmos. Environ.* **2020**, *220*, 117067, doi:10.1016/j.atmosenv.2019.117067.
18. Cheriyan, D.; Choi, J. Estimation of Particulate Matter Exposure to Construction Workers Using Low-Cost Dust Sensors. *Sustain. Cities Soc.* **2020**, *59*, 102197, doi:10.1016/j.scs.2020.102197.
19. Kosmopoulos, G.; Salamalikis, V.; Pandis, S.N.; Yannopoulos, P.; Bloutsos, A.A.; Kazantzidis, A. Low-Cost Sensors for Measuring Airborne Particulate Matter: Field Evaluation and Calibration at a South-Eastern European Site. *Sci. Total Environ.* **2020**, *748*, 141396, doi:10.1016/j.scitotenv.2020.141396.
20. Sousan, S.; Koehler, K.; Thomas, G.; Park, J.H.; Hillman, M.; Halterman, A.; Peters, T.M. Inter-Comparison of Low-Cost Sensors for Measuring the Mass Concentration of Occupational Aerosols. *Aerosol Sci. Technol.* **2016**, *50*, 462–473, doi:10.1080/02786826.2016.1162901.
21. Kaur, K.; Kelly, K.E. Performance Evaluation of the Alphasense OPC-N3 and Plantower PMS5003 Sensor in Measuring Dust Events in the Salt Lake Valley, Utah. *Atmospheric Meas. Tech.* **2023**, *16*, 2455–2470, doi:10.5194/amt-16-2455-2023.

© 2026 by the author(s). Distributed under a Creative Commons CC BY license.

Preprints.org (www.preprints.org) | NOT PEER-REVIEWED | Posted: 17 April 2026 doi:10.20944/preprints202604.1260.v1

22. Cheriyan, D.; Khamraev, K.; Choi, J. Varying Health Risks of Respirable and Fine Particles from Construction Works. *Sustain. Cities Soc.* **2021**, *72*, 103016, doi:10.1016/j.scs.2021.103016.
23. Choi, J.; Khamraev, K.; Cheriyan, D. Hybrid Health Risk Assessment Model Using Real-Time Particulate Matter, Biometrics, and Benchmark Device. *J. Clean. Prod.* **2022**, *350*, 131443, doi:10.1016/j.jclepro.2022.131443.
24. Dong, T.-F.; Sun, W.-Q.; Li, X.-Y.; Sun, L.; Li, H.-B.; Liu, L.-L.; Wang, Y.-; Wang, H.-L.; Yang, L.-S.; Zha, Z.-Q. Short-Term Associations between Ambient PM1, PM2.5, and PM10 and Hospital Admissions, Length of Hospital Stays, and Hospital Expenses for Patients with Cardiovascular Diseases in Rural Areas of Fuyang, East China. *Int. J. Environ. Health Res.* **2025**, *35*, 1059–1071, doi:10.1080/09603123.2024.2380353.
25. Yang, Y.; Ruan, Z.; Wang, X.; Yang, Y.; Mason, T.G.; Lin, H.; Tian, L. Short-Term and Long-Term Exposures to Fine Particulate Matter Constituents and Health: A Systematic Review and Meta-Analysis. *Environ. Pollut.* **2019**, *247*, 874–882, doi:10.1016/j.envpol.2018.12.060.
26. Zheng, T.; Bergin, M.H.; Johnson, K.K.; Tripathi, S.N.; Shirodkar, S.; Landis, M.S.; Sutaria, R.; Carlson, D.E. Field Evaluation of Low-Cost Particulate Matter Sensors in High- and Low-Concentration Environments. *Atmospheric Meas. Tech.* **2018**, *11*, 4823–4846, doi:10.5194/amt-11-4823-2018.
27. Park, S.; Lee, S.; Yeo, M.; Rim, D. Field and Laboratory Evaluation of PurpleAir Low-Cost Aerosol Sensors in Monitoring Indoor Airborne Particles. *Build. Environ.* **2023**, *234*, 110127, doi:10.1016/j.buildenv.2023.110127.
28. Si, M.; Xiong, Y.; Du, S.; Du, K. Evaluation and Calibration of a Low-Cost Particle Sensor in Ambient Conditions Using Machine-Learning Methods. *Atmospheric Meas. Tech.* **2020**, *13*, 1693–1707, doi:10.5194/amt-13-1693-2020.
29. Saputra, C.; Faqiih, M.N.; Thalia, A.F.; Safari, I.A.; Salam, R.A. Calibration of a Low-Cost Particulate Matter Sensor Using the Decay Method. *J. Phys. Conf. Ser.* **2025**, *2942*, 012042, doi:10.1088/1742-6596/2942/1/012042.
30. Chen, C.-C.; Kuo, C.-T.; Chen, S.-Y.; Lin, C.-H.; Chue, J.-J.; Hsieh, Y.-J.; Cheng, C.-W.; Wu, C.-M.; Huang, C.-M. Calibration of Low-Cost Particle Sensors by Using Machine-Learning Method. In Proceedings of the 2018 IEEE Asia Pacific Conference on Circuits and Systems (APCCAS); October 2018; pp. 111–114.
31. Park, D.; Yoo, G.-W.; Park, S.-H.; Lee, J.-H. Assessment and Calibration of a Low-Cost PM2.5 Sensor Using Machine Learning (HybridLSTM Neural Network): Feasibility Study to Build an Air Quality Monitoring System. *Atmosphere* **2021**, *12*, doi:10.3390/atmos12101306.
32. Yadav, K.; Arora, V.; Kumar, M.; Tripathi, S.N.; Motghare, V.M.; Rajput, K.A. Few-Shot Calibration of Low-Cost Air Pollution ($PM_{2.5}$) Sensors Using Meta Learning. *IEEE Sens. Lett.* **2022**, *6*, 1–4, doi:10.1109/LSENS.2022.3168291.
33. Raheja, G.; Nimo, J.; Appoh, E.K.-E.; Essien, B.; Sunu, M.; Nyante, J.; Amegah, M.; Quansah, R.; Arku, R.E.; Penn, S.L.; et al. Low-Cost Sensor Performance Intercomparison, Correction Factor Development, and 2+ Years of Ambient PM2.5 Monitoring in Accra, Ghana. *Environ. Sci. Technol.* **2023**, *57*, 10708–10720, doi:10.1021/acs.est.2c09264.
34. Huang, C.-H.; He, J.; Austin, E.; Seto, E.; Novosselov, I. Assessing the Value of Complex Refractive Index and Particle Density for Calibration of Low-Cost Particle Matter Sensor for Size-Resolved Particle Count and PM2.5 Measurements. *PLOS ONE* **2021**, *16*, e0259745, doi:10.1371/journal.pone.0259745.
35. Hashmy, Y.; Khan, Z.; Hafiz, R.; Younis, U.; Tauqeer, T. MAQ-CaF: A Modular Air Quality Calibration and Forecasting Method for Cross-Sensitive Pollutants 2021.
36. Molina Rueda, E.; Carter, E.; L'Orange, C.; Quinn, C.; Volckens, J. Size-Resolved Field Performance of Low-Cost Sensors for Particulate Matter Air Pollution. *Environ. Sci. Technol. Lett.* **2023**, *10*, 247–253, doi:10.1021/acs.estlett.3c00030.
37. Christakis, I.; Tsakiridis, O.; Kandris, D.; Stavrakas, I. A Kalman Filter Scheme for the Optimization of Low-Cost Gas Sensor Measurements. *Electronics* **2023**, *13*, doi:10.3390/electronics13010025.
38. Priyanka, P.R.; Cheriyan, D.; Choi, J. A Proactive Approach to Execute Targeted Particulate Matter Control Measures for Construction Works. *J. Clean. Prod.* **2022**, *368*, 133168, doi:10.1016/j.jclepro.2022.133168.
39. Plantower PMS5003---Laser PM2.5 Sensor-Plantower Technology Available online: https://www.plantower.com/en/products_33/74.html (accessed on 12 February 2026).

© 2026 by the author(s). Distributed under a Creative Commons CC BY license.

Preprints.org (www.preprints.org) | NOT PEER-REVIEWED | Posted: 17 April 2026 doi:10.20944/preprints202604.1260.v1

40. Alphsense Optical Particle Counter OPC-N3 Available online: https://store.alphasense.com/opc-n3/ (accessed on 12 February 2026).
41. Bohren, C.F.; Huffman, D.R. *Absorption and Scattering of Light by Small Particles*; John Wiley & Sons, 2008; ISBN 978-3-527-61816-3.
42. Sousan, S.; Regmi, S.; Park, Y.M. Laboratory Evaluation of Low-Cost Optical Particle Counters for Environmental and Occupational Exposures. *Sensors* **2021**, *21*, doi:10.3390/s21124146.
43. Hastie, T.; Tibshirani, R.; Friedman, J. *The Elements of Statistical Learning*; Springer Series in Statistics; Springer: New York, NY, 2009; ISBN 978-0-387-84857-0.

Disclaimer/Publisher's Note: The statements, opinions and data contained in all publications are solely those of the individual author(s) and contributor(s) and not of MDPI and/or the editor(s). MDPI and/or the editor(s) disclaim responsibility for any injury to people or property resulting from any ideas, methods, instructions or products referred to in the content.

© 2026 by the author(s). Distributed under a Creative Commons CC BY license.